The Journal of Experimental Biology 214, 1533-1545

doi:10.1242/jeb.053165

RESEARCH ARTICLE

Physiological responses of the scleractinian coral *Pocillopora damicornis* to bacterial stress from *Vibrio coralliilyticus*

Jeremie Vidal-Dupiol[1,*], Ophélie Ladrière[2,*], Anne-Leila Meistertzheim[1], Laurent Fouré[3], Mehdi Adjeroud[4] and Guillaume Mitta[1,†]

[1]UMR 5244, CNRS UPVD EPHE, Université de Perpignan Via Domitia, 52 Avenue Paul Alduy, 66860 Perpignan Cedex, France, [2]Unité d'écologie marine, Laboratoire d'écologie animale et écotoxicologie, Université de Liège, 15 Allée du 6 août, Bat. B6C, 4000 Liege, Belgium, [3]Aquarium du Cap d'Agde, 11 rue des 2 frères, 34300 Cap d'Agde, France and [4]Institut de Recherche pour le Développement, Unité 227 CoRéUs2 "Biocomplexité des écosystèmes coralliens de l'Indo-Pacifique", bp A5, 98848 Nouméa Cedex, Nouvelle-Calédonie

*These authors contributed equally to this work
†Author for correspondence (mitta@univ-perp.fr)

Accepted 19 January 2011

SUMMARY

As the effects of climate change have become increasingly visible over the past three decades, coral reefs have suffered from a number of natural and anthropogenic disturbances that have caused a critical decline in coral populations. Among these disturbances are coral diseases, which have appeared with increasing frequency and severity, often in correlation with increases in water temperature. Although the crucial role played by *Vibrio* species in coral disease has been widely documented, the scientific community does not yet fully understand the infection process of *Vibrio* or its impact on coral physiology and immunology. Here, we investigated the physiological and transcriptomic responses of a major reef-building coral, *Pocillopora damicornis*, when exposed to a specific pathogen (*Vibrio coralliilyticus*) under virulent (increasing water temperature) and non-virulent (constant low temperature) conditions. The infection process was examined by electron microscopy and quantitative reverse-transcription PCR, and coral health was monitored by visual observations and measurements of zooxanthellar density. The results obtained suggest that coral tissue invasion occurs upon increasing water temperature only. Transcriptomic variations were investigated using a suppression–subtractive–hybridization approach, and the expression levels of six candidate immune-related genes were examined during bacterial exposure. These genes correspond to three lectin-like molecules putatively involved in the recognition of pathogens, two metal-binding proteins putatively involved in antibacterial response and one cystein protease inhibitor. The transcription patterns of these selected genes provide new insights into the responses of coral colonies to virulent *versus* non-virulent bacteria.

Supplementary material available online at http://jeb.biologists.org/cgi/content/full/214/9/1533/DC1

Key words: *Pocillopora damicornis*, *Vibrio coralliilyticus,* biomarker, coral disease, global change, vibriosis.

INTRODUCTION

Coral reef ecosystems are among the most biologically diverse and complex marine ecosystems worldwide. In addition to their biological and ecological importance, coral reefs support major economic and physical functions (e.g. food production, tourism, biotechnology development and coast protection) that are essential for many countries (Lesser, 2004). These ecosystems are principally supported by small, colonial and calcifying organisms, the hermatypic scleractinian corals, which enter into mutualistic symbioses with microalgae of the genus *Symbiodinium*, dinoflagellates that are also referred to as zooxanthellae (Lesser, 2004).

Because of global climate change and anthropogenic pressure, coral reef ecosystems have been increasingly confronted with severe natural and anthropogenic disturbances over the past three decades (Hughes et al., 2003; Ward and Lafferty, 2004; Donner et al., 2005; Hoegh-Guldberg et al., 2007; Bourne et al., 2009). A recent global assessment of coral reef health showed that approximately 19% of coral reefs were irremediably degraded with no sign of recovery, 15% presented symptoms of an imminent risk of collapse and another 20% were at risk of becoming critically affected in the next few decades (Wilkinson, 2008). Coral diseases are among the major factors in coral reef degradation; their impacts have severely increased in recent decades, in apparent association with global climate change (Weil et al., 2006; Bourne et al., 2009). Indeed, it has been suggested that high temperatures influence the outcome of bacterial infections by lowering the disease resistance of corals and/or increasing pathogen growth, virulence and infectivity (Ward et al., 2007; Rodriguez-Lanetty et al., 2009).

To date, 18 coral diseases have been identified (Sutherland et al., 2004; Willis et al., 2004; Harvell et al., 2007). Among the well-characterized coral infectious diseases, several have been shown to be caused by members of the Vibrionaceae family (Kushmaro et al., 2001; Ben-Haim et al., 2003a; Sussman et al., 2008). Bacteria belonging to the genus *Vibrio* are ubiquitously distributed in aquatic environments worldwide, from brackish water to deep-sea environments. Kushmaro et al. demonstrated that the bacteria *Vibrio shiloi* infects and triggers bleaching of the coral *Oculina*

patagonica (Kushmaro et al., 1996; Kushmaro et al., 1997; Kushmaro et al., 1998; Kushmaro et al., 2001). The same research group showed that the infectivity of this bacteria is temperature dependent and occurs only after an increase in seawater temperature (Kushmaro et al., 1998). A similar temperature-dependent virulence was observed in interactions between *Vibrio coralliilyticus* and the scleractinian coral *Pocillopora damicornis* (Ben-Haim et al., 2003b), and the involvement of *Vibrio* species has been suggested in two other coral diseases: yellow blotch/band disease (Cervino et al., 2004; Cervino et al., 2008) and rapid tissue necrosis (Luna et al., 2007). Among these *Vibrio*-related diseases, the bleaching disease of *O. patagonica* caused by the infection of *V. shiloi* has been characterized to the greatest degree (for a review, see Rosenberg, 2004). In brief, *V. shiloi* is attracted by chemotaxis and adheres to β-galactoside-containing receptors on coral cells. This adhesion process is specific and dependent on temperature: no adhesion occurs at low temperatures (16–20°C), whereas *V. shiloi* actively adhere to their target at temperatures between 25 and 30°C. After contact, the bacteria penetrate and multiply within the coral cells, and begin producing two sets of factors: extracellular proline-rich toxins (referred to as toxin P) (Banin et al., 2001) that block photosynthesis, and enzymes that trigger the lysis of zooxanthellae.

However, although *Vibrio* species have been shown to play crucial roles in several coral diseases, our knowledge of the effects of *Vibrio* infection on coral physiology remains incomplete. Accordingly, the present study used a global transcriptomic approach to examine the physiological responses of coral colonies when confronted with bacterial stress and/or infection in a realistic ecological context. Specifically, we studied the interaction between the coral *P. damicornis* and its specific pathogenic bacteria, *V. coralliilyticus*.

Pocillopora damicornis has a widespread distribution in the Indo-Pacific region (Veron, 2000), is highly sensitive to a wide range of natural and anthropogenic disturbances, and is a good sentinel species for use in monitoring coral reef health (Gates et al., 1992; Ben-Haim and Rosenberg, 2002; Stimson et al., 2002; Hashimoto et al., 2004; Vidal-Dupiol et al., 2009). *Vibrio coralliilyticus* is a specific pathogen of *P. damicornis*, and its virulence is temperature dependent; the bacterium has been shown to trigger coral bleaching at moderate temperatures (24–25°C) and coral tissue lysis at higher temperatures (26–29°C) (Ben-Haim Rozenblat and Rosenberg, 2004). Consequently, the *P. damicornis*–*V. coralliilyticus* model allows us to compare coral responses to virulent and non-virulent bacteria.

Here, we exposed coral to a consistent supply of bacteria at either 25°C (non-virulent) or under conditions of a gradual temperature increase (from 25 to 32.5°C; induction of virulence) and examined transcriptomic modifications using subtractive hybridization. The differentially regulated genes identified through this approach included several thought to be involved in immune processes. Quantitative reverse-transcription PCR (qRT-PCR) was used to follow the expression levels of a number of selected genes at various time points after the onset of bacterial stress or infection.

MATERIALS AND METHODS

Biological materials

The *Pocillopora damicornis* (Linnaeus 1758) isolate used in this study was harvested in Lombock, Indonesia (CITES no. 06832/VI/SATS/LN/2001) and maintained at the Cap d'Agde Aquarium, France. For experimental procedures, nubbins (10 g; 7×6 cm height×diameter) were propagated by cutting branches from the parent colony and physiologically stabilizing them for 2 months at 25°C.

The coral pathogen *Vibrio coralliilyticus* strain YB1 (Ben-Haim et al., 2003a) (CIP 107925, Institut Pasteur, Paris, France) was used to challenge or infect *P. damicornis* (Ben-Haim and Rosenberg, 2002). *Vibrio coralliilyticus* was cultured in 2216 Marine Broth medium (catalog no. 279110; BD Difco, Le Pont de Claix, France) under aerobic conditions with shaking (150 rpm) at 30°C for routine use, or at the temperature in the coral-containing tank for the Tb and Cb groups (see Experimental infection).

Experiments aimed at determining which cells (host or symbiont) expressed the candidate genes (see Identification of host or symbiont genes) utilized three zooxanthellar isolates corresponding to clonal cultures of zooxanthellae from the B, C and D clades (BURR Culture Collection, University of Buffalo; culture IDs Flap3, Pd44b and MF2.2b, respectively). The representative zooxanthellae were cultured in 250 ml screw-top polycarbonate cell-culture flasks (Corning, Paris, France) in filtered seawater (pore size, 0.2 μm) enriched with 1× Guillard's (F/2) marine water enrichment solution (Sigma-Aldrich, Lyon, France) and supplemented with 1× antibiotic/antimycotic stabilized suspension (Sigma-Aldrich). The zooxanthellae were grown at 25±1°C under an irradiance of 70 μmol photons m^{-2} s^{-1} provided by daylight fluorescent tubes (Sylvania, Gennevilliers, France) set to a 12 h:12 h light:dark photoperiod. Stock cultures were transferred monthly, and cells were used in the stationary phase.

Experimental infection

Bacterial challenge was induced by constantly supplying *V. coralliilyticus* at a relatively low temperature (25°C; non-virulent), whereas infection was induced by constantly supplying the bacteria and systematically increasing the water temperature from 25 to 32.5°C (thereby activating bacterial virulence).

Bacterial challenge, bacterial infection and their respective controls were established in four independent tanks: (1) constant low temperature (25°C) and bacterial supply (Cb); (2) gradual temperature increase from 25 to 32.5°C and regular bacterial supply (Tb); (3) constant low temperature without bacteria (C); and (4) gradual temperature increase from 25 to 32.5°C in the absence of bacteria (T). For experiments, nubbins of *P. damicornis* were randomly placed in 1201 tanks (N=27 per tank). After a 14-day acclimatization at 25°C, the C and Cb treatments were maintained at this temperature whereas the temperatures of the T and Tb treatments were gradually increased by 1.5°C every 3 days until the water temperature reached 32.5°C (days 3, 6, 9, 12 and 15). This higher temperature was maintained until the corals bleached or lysed. In the Cb and Tb treatments, bacteria (10^3 cells ml^{-1} of tank water) were supplied by balneation (Ben-Haim Rozenblat and Rosenberg, 2004). The first bacterial supply was initiated on day 1 and repeated every 3 days (days 1, 4, 7, 10, 13, 16 and 19). The utilized cultures of *V. coralliilyticus* were prepared at 25°C for the Cb treatment and at the temperature corresponding to the tank temperature for the Tb treatment. For the Tb and T treatments, beginning on day 3, the temperature was increased by +1.5°C every 3 days until it reached 32.5°C.

Three nubbins were randomly sampled from each tank every 3 days (days 0, 3, 9, 12, 15 and 18). Five 0.5-cm apices were cut from each nubbin; three were immediately frozen and stored in liquid nitrogen for later measurement of zooxanthellar density and two were fixed directly in 2.5% glutaraldehyde and subjected to electron microscopy.

The tank temperature was controlled using an aquarium heater (600 W, Schego, Offenbach, Germany) connected to an electronic thermostat (Hobby Biotherm Professional, Koblenz, Germany).

Illumination was supplied at an irradiance of 250 µmol photons m^{-2} s^{-1} (quantum meter; QMSW-SS, Apogee Instruments Inc., Roseville, CA, USA) by metal halide lamps (400 W, Iwasaki 6500 Kelvin, Tokyo, Japan) set to a 12 h:12 h light:dark photoperiod. All other seawater parameters were maintained constant over time and between tanks. A constant water flow was maintained within each tank using a water pump (1300 l h^{-1}, IDRA, Pozzoleone, Italy). Seawater was continuously recycled at a rate of 10.8 tank volumes per hour by coupling the action of a biological filter and an Aquavie protein skimmer (EPS 600, Montpellier, France), and the water was renewed (2% tank volume per day) with natural filtered Mediterranean seawater heated to 25°C. To avoid the growth of bacterial blooms, the water was continuously treated using a UVC filter (5 W, AquaCristal Series II, JBL, Neuhofen, Germany). During bacterial balneation, all equipment known to remove or kill bacteria (e.g. the protein skimmer and UVC filter) were inactivated for the first 4 h after treatment, allowing the bacteria to adhere to the coral tissues.

In order to monitor coral health, physiological (e.g. zooxanthellar density measure) and visual (e.g. coral color, tissue lysis appearance, opened or closed polyps) measurements were performed throughout the experiments. Zooxanthellar density was used as a measurement of coral health and the stability/breakdown of symbiosis. Coral tissues were extracted using a water pick (Johannes and Wiebe, 1970) in 50 ml of filtered seawater (0.2 µm pore size), homogenized with a Potter grinder and fixed with 2% formaldehyde. Zooxanthellae were counted under a light microscope using a hemocytometer, and algal densities were standardized per skeletal surface area, as described previously (Stimson and Kinzie, 1991). Every day, two colonies per tank (the same colonies each day) were photographed using a consistent camera setup, and both bleaching and lytic events were thoroughly examined.

Bacteria and the infectious process

In order to follow the infectious process in *P. damicornis* tissues, the presence of *V. coralliilyticus* was investigated by transmission electron microscopy (TEM). Two ultrathin slices were prepared from coral fragments fixed in 2.5% glutaraldehyde in filtered seawater (0.2 µm pore size). Sections were prepared as described previously (Ladrière et al., 2008) and observed with a Jeol JEM 100-SX transmission electron microscope (JEOL, Zaventem, Belgium) at an accelerating voltage of 80 kV.

qRT-PCR was used to quantify the amount of *V. coralliilyticus* present in *P. damicornis* tissues. Total RNA was extracted from each sample (see Subtractive cDNA library construction) and 100 ng of total RNA were reverse transcribed using hexamer primers and a RevertAid™ kit (Fermentas International Inc., Saint-Rémy-lès-Chevreuse, France). qRT-PCR was performed with 4 µl cDNA (1/100 dilution) in a total volume of 10 µl using a LightCycler 480 System (Roche Diagnostics, Meylan, France), as described below (see Real-time analysis). Oligonucleotide primers were designed based on the aligned sequences from eight different *V. coralliilyticus* 16S rRNAs (GenBank accession nos EF094886, DQ079633, GQ406805.1, GQ406804.1, GQ406802.1, GQ406801.1, GQ406800.1 and GQ406798.1; National Center for Biotechnology Information database) and the 28S rRNA of *P. damicornis* (Vidal-Dupiol et al., 2009) (Table 1). RNA extracted from the *V. coralliilyticus* culture used for infection was taken as the positive control. The qRT-PCR products were cloned and sequenced (see DNA sequencing and sequence analysis).

Subtractive cDNA library construction

Visual and physiological monitoring was used to select early bacterially stressed or infected samples, and subtractive hybridization was used to identify genes that were differentially expressed under the non-virulent and virulent conditions. For each set of three nubbins, tissues were extracted with a water pick in 800 ml of filtered seawater (0.2 µm pore size), and both total RNA and mRNA were purified (Vidal-Dupiol et al., 2009). Forward and reverse suppression–subtractive–hybridization (SSH) libraries were constructed using the PCR-Select cDNA Subtraction kit (Clontech, Saint-Germain-en-Laye, France). Tester and driver cDNA were prepared using 2 µg of Poly(A)+ RNA, and enzyme digestion, adaptor ligation, hybridization and PCR amplification were performed according to the manufacturer's instructions (Clontech). The resulting PCR products were cloned into pCR4-TOPO using a TOPO TA cloning kit (Invitrogen, Cergy Pontoise, France) and transformed into One Shot TOP10 chemically competent *Escherichia coli* cells (Invitrogen).

DNA sequencing and sequence analysis

For each library, 384 clones were randomly selected and single-pass sequenced by GATC Biotech, using an ABI 3730xl apparatus. Vector and adaptor sequences were trimmed from all sequences using Sequencher™ software (Gene Codes Corp., Ann Arbor, MI, USA). High-quality expressed sequence tags (ESTs) (>100 bp) were assembled into clusters or identified as unique sequences, and used for database searches with the BLASTX and BLASTN programs. Specific domain searches were performed using the InterProscan software. ESTs displaying significant similarities with a gene of known function were assigned to the appropriate functional class. The various EST sequences have been submitted to the dbEST database; in an effort to minimize redundancy, sequences displaying 100% identity with one another were submitted as a single sequence.

Table 1. Combinations of forward and reverse primers used in real-time PCR expression analysis

Gene name	Forward primer (5′→3′)	Reverse primer (5′→3′)
Concanavalin	CATCTCCGTCCCAAAC	CAACTGCATAATGAACCCA
Cystatin B	ATGGCCTTCCTTCTTTG	AGGTGTATGTGGGTGAC
Ferritin	AGAATATGCGGGGAGG	CCTGGACCAACACGAG
Major basic nuclear protein	GGTACAGCAAACTGCG	TTGGAAACGTCCGACC
PdC-lectin	ATTGGCAGAACGGAAG	GGGAGGAGACCTGGTA
P-selectin	CAATGTTATCATTACCGACCC	GTCTGTTCCAGTCCAGG
Selenium binding protein	TACGCCTTCCGGTAAC	GTTCTACCCTGACCTGG
60S ribosomal protein L40A	CGACTGAGAGGAGGAGC	CTCATTTGGACATTCCCGT
60S ribosomal protein L22	TGATGTGTCCATTGATCGTC	CATAAGTAGTTTGTGCAGAGG
60S acidic ribosomal phosphoprotein P0	GCTACTGTTGGGTAGCC	CTCTCCATTCTCGTATGGT
Vibrio coralliilyticus 16S rRNA	TTAAGTAGACCGCCTGGG	GATGTCAAGAGTAGGTAAGGTTC
Pocillopora damicornis 28S rRNA	CGGGTGAGAATCCTGT	CTGAAGGCCATCCTCAA

qRT-PCR analyses

qRT-PCR was used to analyze the expression profiles of selected genes. Total RNA was extracted, and this total RNA (2.5 µg) was reverse transcribed using oligo dT primers and the Superscript II enzyme (Invitrogen). The resulting cDNA products were purified using a Nucleotrap Gel Extraction Trial kit (Clontech), and qRT-PCR was performed with 2.5 µl of purified cDNA (diluted 1:50 in water) in a total volume of 10 µl containing 1× LightCycler® 480 SYBR Green I Master Mix (Roche Diagnostics) and 70 nmol l^{-1} of each primer. The primers, which were designed using Light Cycler Probe Design Software version 1.0 (Roche Diagnostics), are presented in Table 1. Amplification was performed using a LightCycler 480 System (Roche Diagnostics) and the following reaction conditions: activation of the Thermo-Start® DNA polymerase at 95°C for 15 min, followed by 45 cycles of denaturation at 95°C for 30 s and annealing/extension at 60°C for 1 min. Melting curve profiles (95 to 70°C decreasing by 0.5°C every 10 s) were assayed to ensure that we were looking at a single product. Each run included a positive cDNA control that was sampled at the beginning of the experiment (day 0) and also from each amplification plate; this positive control was also used as the calibrator sample, and blank controls (water) were included for each primer pair. The PCR products were resolved by electrophoresis, the bands were isolated directly from agarose gels and DNA was extracted using the Gel Extraction PCR Purification System V (Promega, Charbonnières-les-Bains, France). The resulting qRT-PCR products were single-pass sequenced as described above.

For each reaction, the crossing point (C_p) was determined using the second derivative maximum method applied using Light Cycler Software version 3.3 (Roche Diagnostics). The PCR efficiency (E) of each primer pair was calculated by determining the slope of standard curves obtained from serial-dilution analysis of cDNAs pooled from all experimental samples, as described by Yuan et al. (Yuan et al., 2006). The individual qRT-PCR efficiencies for the target or reference genes were calculated using the formula: $E=10^{(-1/\text{slope})}$. For each candidate gene, the level of transcription was normalized using the mean geometric transcription rate of three reference sequences encoding ribosomal protein genes from the host, *P. damicornis*: *60S ribosomal protein L22*, *60S ribosomal protein L40A* and *60S acidic ribosomal phosphoprotein P0* (GenBank accession nos HO112261, HO112283 and HO112666, respectively). The normalized relative quantities (NRQs) were calculated as described by Hellemans and colleagues (Hellemans et al., 2007), using the equation:

$$NRQ = \frac{E_{\text{target}}^{\Delta C_{\text{p,target}}}}{\sqrt[3]{\prod_{i=1}^{3} E_{\text{ref}_i}^{\Delta C_{\text{p,ref}_i}}}},$$

where E_{target} is the amplification efficiency of the gene of interest; E_{ref} is the amplification efficiency of the reference gene; $\Delta C_{\text{p,ref}}=C_{\text{p,ref}}(\text{calibrator})-C_{\text{p,ref}}(\text{sample})$; and $\Delta C_{\text{p,target}}=C_{\text{p,target}}(\text{calibrator})-C_{\text{p,target}}(\text{sample})$.

Identification of host or symbiont genes

To determine which organism (host or symbiont) expressed the candidate genes, cross-PCR experiments were performed on DNA and RNA extracted from the holobiont (host plus symbiont) and from pure cultured zooxanthellae, as previously described (Vidal-Dupiol et al., 2009). Briefly, PCR amplifications were performed with oligonucleotides amplifying the targets, the gene encoding the small ribosomal subunit RNA *Symbiodinium* spp. (Rowan and Powers, 1991) and the cDNA encoding the major basic nuclear protein (MBNP) of *Symbiodinium* spp. (Table 1).

Statistical analysis

Because conditions of normality and homoscedasticity were not satisfied, within-set variations in zooxanthellar density were analyzed with the non-parametric Kruskal–Wallis (KW) test using GraphPad InStat 3 (GraphPad Software, La Jolla, CA, USA). Variations in gene expression over time were analyzed with a maximum normed residual test (Grubbs, 1969; Stefansky, 1972) using JMP (SAS Institute, Inc., Cary, NC, USA). Analyses were performed on qRT-PCR results obtained for a double-passed pool of three nubbins from the same treatment at each sampling date. Differences were considered statistically significant at $P<0.05$.

RESULTS

Coral health and infection status

In order to investigate the effect of bacterial challenge and/or infection, we designed two sets of experiments. The first set examined the effects of non-virulent bacterial challenge by *V. coralliilyticus*. A constant temperature of 25°C was used, as exposure of *P. damicornis* to *V. coralliilyticus* at this temperature was previously shown to trigger bleaching without tissue lysis (Ben-Haim Rozenblat and Rosenberg, 2004). Tanks were maintained at 25°C with (Cb) and without (C) bacteria (10^3 bacteria ml^{-1}). In the second set of experiments, which examined the effects of infection by virulent bacteria, a similar setup was used, except that the tanks with (Tb) and without (T) bacteria were subjected to a gradual temperature increase from 25 to 32.5°C. At each time point, the bacteria added to Tb were cultured at the tank temperature.

Coral health and the stability/breakdown of symbiosis were examined by analysis of zooxanthellar density and visual monitoring. For the C and Cb treatments, the zooxanthellar densities (cells cm^{-2} of skeleton) remained stable throughout the experiment (mean±s.d.: $C=1.07\times10^6\pm2.35\times10^5$ and $Cb=5.18\times10^5\pm2.89\times10^5$ cells cm^{-2}). There was no significant difference in zooxanthellar density between C and Cb (KW, $P>0.05$), indicating that bleaching did not occur under these experimental conditions. For the T and Tb treatments, the zooxanthellar densities remained stable over the first 15 days (mean±s.d.: $T=6.21\times10^5\pm1.61\times10^5$ and $Tb=4.36\times10^5\pm1.69\times10^5$ cells cm^{-2}), but dropped to $6.26\times10^3\pm5.05\times10^3$ and $1.72\times10^5\pm6.23\times10^4$ cells cm^{-2}, respectively, by day 18. This decrease was only significant for the Tb treatment (KW; $P=0.0535$ and $P=0.0147$ for T and Tb, respectively).

Visual monitoring was used to follow the occurrence of symptoms such as tissue lysis and/or bleaching. In the C and Cb treatments, the nubbins appeared healthy throughout the duration of the experiment (Fig. 1). In the tank subjected to only increased temperature (T treatment), polyps were closed at day 15, bleaching became visible in the upper portion of nubbins at day 16 and bleaching was complete by day 18 (Fig. 1). These bleached corals were pale but still alive; when the tank temperature was returned to 25°C, the polyps reopened (Fig. 2). In the Tb treatment, however, tissue lysis was first observed on day 12; lytic plaques were observed in the coral tissues and calcified skeletons (seen at the beginning as small white spots) became evident on the nubbins (Fig. 2). This effect continued until lysis was complete (Fig. 1; day 21). In order to confirm that corals subjected to bacterial infection were dead, the tank temperature was returned to 25°C. After several days at this temperature, polyps did not reopen and the skeleton began to be colonized by algae.

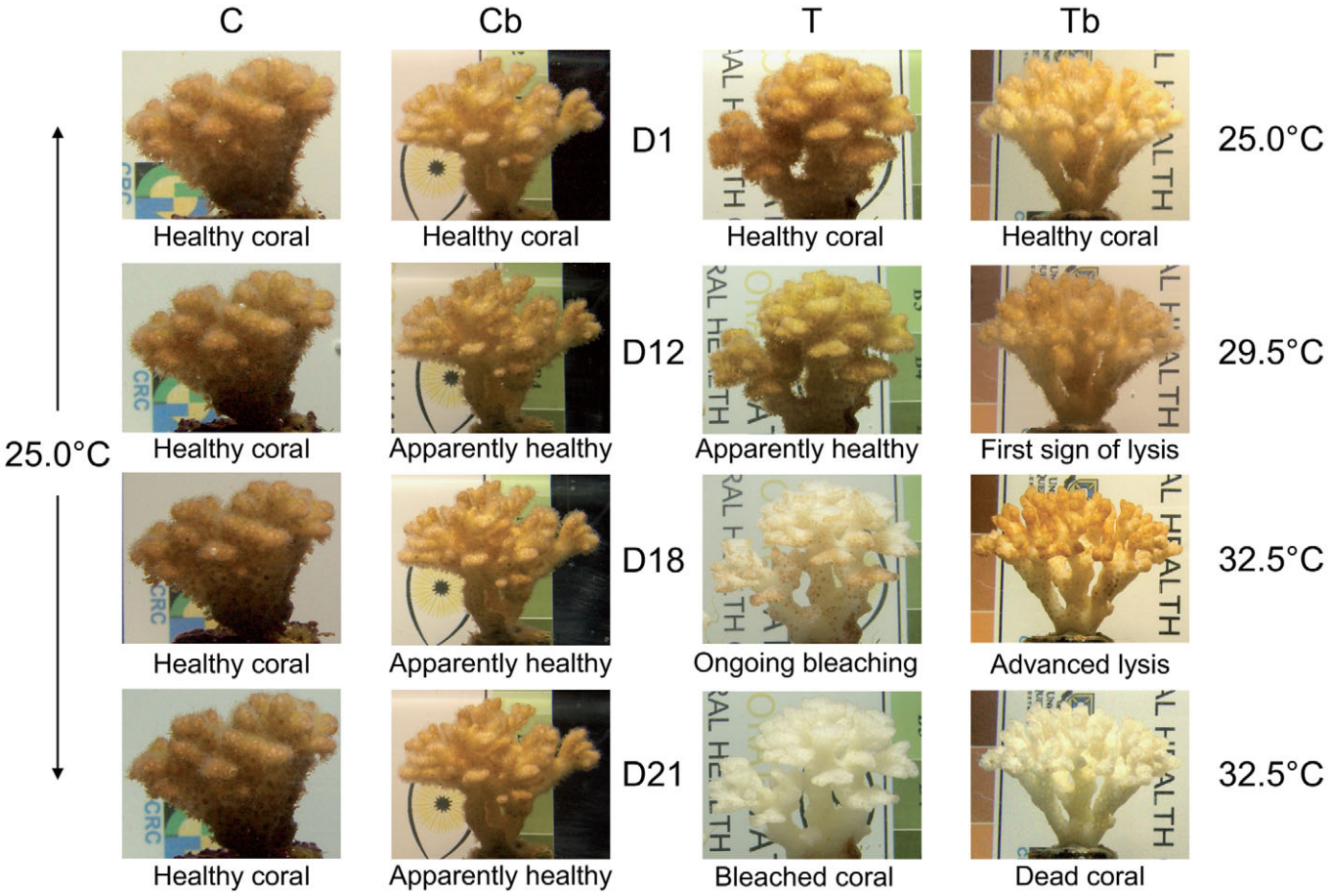

Fig. 1. Visual monitoring. Photos of *Pocillopora damicornis* nubbins taken at various time points during the experiment from treatments C (25°C without bacterial balneation), Cb (25°C with bacterial balneation), T (temperature increasing from 25 to 32.5°C without bacterial balneation) and Tb (temperature increasing from 25 to 32.5°C with bacterial balneation).

In order to substantiate that *V. coralliilyticus* was responsible for the observed symptoms, three randomly chosen samples were harvested from each tank at each time point, and the presence/amount of bacteria was investigated using electron microscopy and qRT-PCR. Tb samples showed no bacteria during the first 6 days. On day 9, bacterial aggregates (bacteriocyte-like structures) were first detected inside the ectodermal host cells (Fig. 3A). Similar aggregates were reported by Ben-Haim et al. (Ben-Haim et al., 2003b) when sections of *P. damicornis* infected by *V. coralliilyticus YB1* were analyzed using the same methodology. This suggests that the bacteria multiply inside the ectoderm before tissue lysis becomes visible to the naked eye. Three days later (day 12, 29.5°C, Fig. 3B–D), the tissues surrounding the bacteriocyte-like structures were disorganized and most cellular organelles were lysed (Fig. 3B,C). In contrast, identically treated and processed samples from the other treatments (C, Cb and T) failed to show any bacterial aggregates or lytic events during the experimental period.

To confirm that the observed bacteria were not opportunistic bacteria of another species, we used qRT-PCR to quantify the levels of the *V. coralliilyticus* 16S rRNA in the tissue samples. *Vibrio coralliilyticus*-specific primers were designed and used for amplification of cDNA, and the levels of *V. coralliilyticus* 16S rRNA were compared to that of the *P. damicornis* 28S rRNA. *V. coralliilyticus* 16S rRNA corresponding amplicons were cloned and 40 randomly picked clones were sequenced. All sequences obtained corresponded to the *V. coralliilyticus* 16S rRNA. Consistent with the above results, qRT-PCR showed that the relative amount of *V. coralliilyticus* 16S rRNA increased significantly by day 6 and remained higher than the control until the end of the protocol (Fig. 4). By comparison, no such increase was observed in Cb group (Fig. 4). This strongly suggests that coral tissue invasion occurs upon increasing water temperature only.

EST sequencing, general features and functional classification of the BI, BR, TBI and TBR libraries

Two SSH experiments were performed to monitor the coral response to bacterial challenge or infection. The first was conducted using pooled samples (days 12 and 15) from the Cb treatment *versus* the C treatment, whereas the second was conducted using pooled samples (days 9–15) from the Tb treatment *versus* the T treatment. This yielded four cDNA libraries: the bacteria-induced (BI) and bacteria-repressed (BR) libraries, which corresponded to the subtractive hybridization of Cb *versus* C, and the thermo-bacteria-induced (TBI) and thermo-bacteria-repressed (TBR) libraries, which corresponded to the subtractive hybridization of Tb *versus* T. The 'induced' libraries contained transcripts putatively induced by bacterial stress or infection whereas the 'repressed' libraries contained gene putatively downregulated under the experimental conditions.

The general features of each library are given in Table 2. Three hundred and eighty-four clones were sequenced from each library,

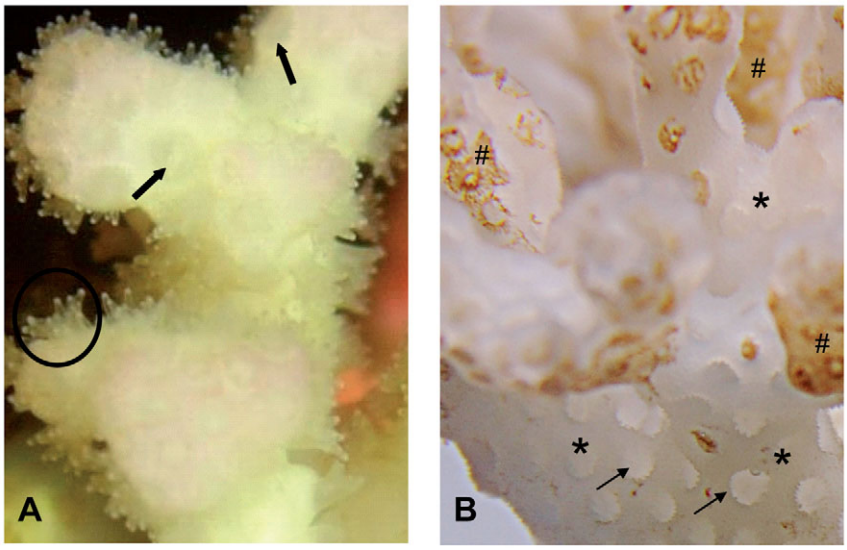

Fig. 2. Enlargement of photos of *P. damicornis* nubbins subjected to (A) thermal bleaching (T treatment) or (B) bacterial lysis (Tb treatment). (A) Nubbins 3 days after the end of the T treatment (day 24). Water temperature was decreased to 25°C on day 21, which led the polyps to reopen. A bleached open polyp is shown (surrounded by a circle). Corallites (e.g. skeleton structure containing a polyp) are indicated by bold arrows. (B) Nubbins at day 20 after the Tb experiment, when coral tissues were quasi-totally lysed. Empty corallites are indicated by arrows. Asterisks mark a portion of bare skeleton; sharps indicates tissue rests undergoing lysis.

yielding 279, 276, 275 and 229 high-quality cDNA sequences (>100 bp) from the BI, BR, TBI and TBR libraries, respectively (Table 2). The ESTs from the BI library coalesced into 63 contigs and 123 singletons, suggesting that the overall redundancy of the library was approximately 56%. The BR, TBI and TBR ESTs distributed to 59, 38 and 23 contigs and 149, 184 and 166 singletons, for overall redundancies of 46, 33 and 28%, respectively (Table 2).

Singleton and consensus clusters were subjected to BLASTN and BLASTX searches and classified into three groups: unknown genes, genes of unknown function, and genes of known function (Fig. 5). Most of the sequences of known gene function presented similarities to predicted proteins from the genomes of *Nematostella vectensis* (an aposymbiotic cnidarian) and *Branchiostoma floridae* (Cephalochordata), both of which have recently been sequenced (Putnam et al., 2007; Putnam et al., 2008). The putative functions of these sequences were deduced by domain analysis using the InterProscan program. The identified genes clustered into the following 13 functional categories: apoptosis, cellular homeostasis, cellular metabolism, chromatin remodeling, cytoskeletal organization, immune responses, intracellular protein transport, photosynthetic processes, protein metabolism, stress responses, RNA metabolism,

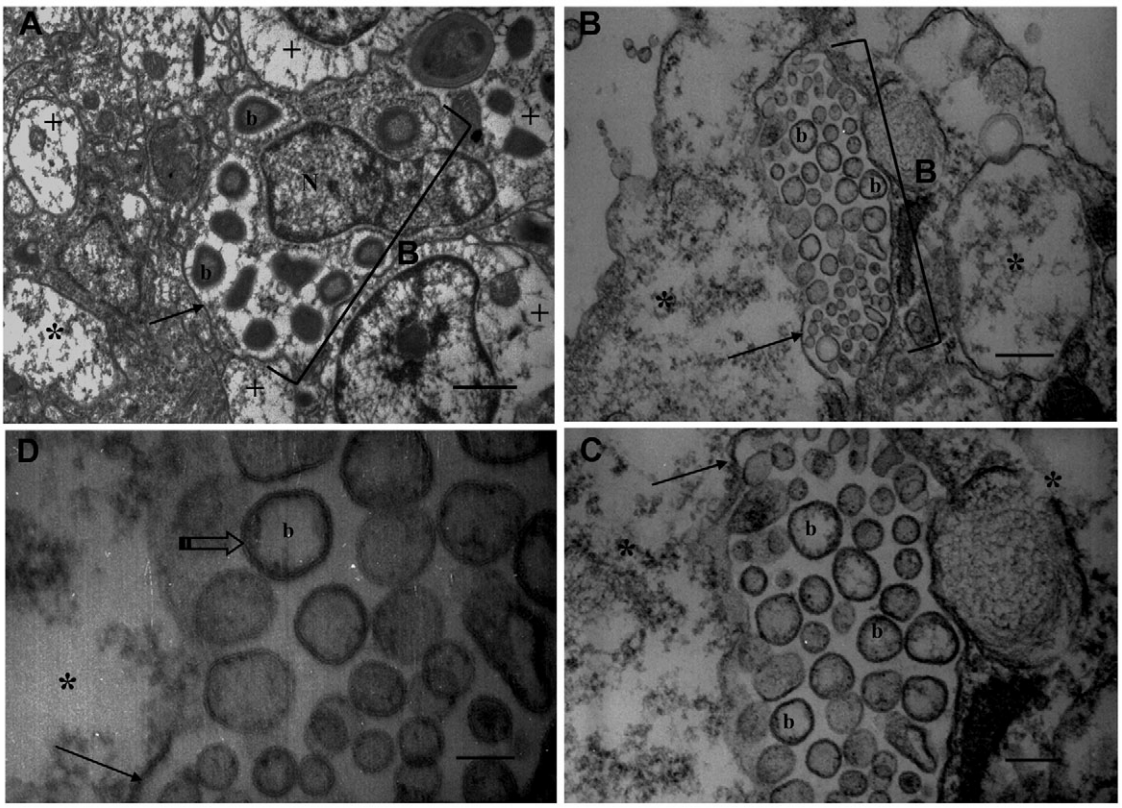

Fig. 3. Electron microscopic monitoring. (A) Thin section of *P. damicornis* sampled from the Tb treatment on day 9. (B) Thin section of *P. damicornis* sampled from the Tb treatment on day 12. (C) Enlargement of B. (D) Enlargement of C. B, bacterial aggregate; b, bacteria; arrows, host cell membrane; cross, tissue disorganization; star, area of strong tissue disorganization and lysis; open arrow, double membrane (bacterial cell wall and cytoplasmic membrane). Scale bars: (A) 1 μm, (B) 500 nm, (C) 250 nm, (D) 125 nm.

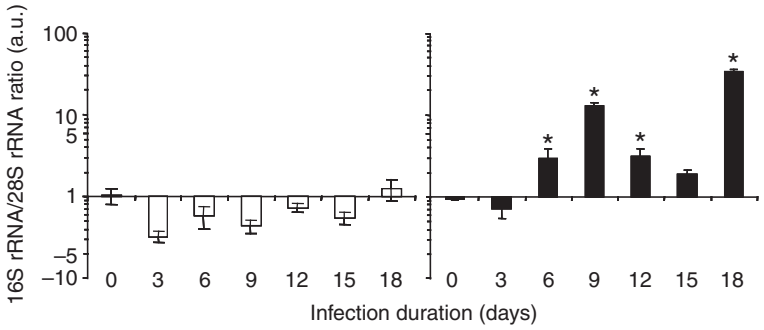

Fig. 4. qRT-PCR quantitation of *Vibrio coralliilyticus* in *P. damicornis* tissues. The relative expression of *V. coralliilyticus* 16S rRNA was normalized with respect to that of *P. damicornis* 28S rRNA. Open and filled histograms correspond to the non-virulent and virulent experiments, respectively.

signal transduction and system development (Fig. 5, supplementary material Table S1).

Expression patterns of genes putatively involved in immune processes during *Vibrio* challenge

To investigate the response of coral to virulent and non-virulent bacterial challenges, five candidate genes were selected from the SSH libraries, and their transcription levels at various post-challenge time points were measured by qRT-PCR (Fig. 6Aii–vi). Three were selected because of their putative involvements in antibacterial responses; these comprised a ferritin-like protein from the TBI library (similar to *Periserrula leucophryna* ferritin; $E=2\times10^{-66}$), a selenium-binding-protein-like protein from the BI library (similar to *Mus musculus* selenium binding protein; $E=2\times10^{-25}$) and a cystatin B-like protein from the BR library (similar to *Danio rerio* cystatin B; $E=4\times10^{-7}$). The other two selected genes, both lectin-like molecules, were selected based on the importance of lectins in invertebrate immunity. They included a P-selectin-like protein from the TBR library (similar to *Homo sapiens* P-selectin; $E=6\times10^{-28}$) and a concanavalin A lectin/glucanase-like protein from the TBI library (similar to *Synechococcus* sp. thrombospondin N-terminal-like domain-containing protein; $E=2\times10^{-9}$). These candidates were classified as lectins because the InterProscan analysis of their translated amino-acid sequences revealed the presence of a concanavalin A-like lectin/glucanase domain (InterProscan accession no. SSF49899) and a P-selectin-like domain (InterProscan accession no. PR00343), both of which contain carbohydrate-binding sites. Following our recent discovery in a previous study of another lectin from *P. damicornis*, PdC-lectin (Vidal-Dupiol et al., 2009), we further investigated the transcript variation of this third lectin under the same experimental conditions (Fig. 6Ai). To verify that the observed variations were linked to the targeted physiological effects and not to profound bacteria-induced disturbances, we also examined the expression levels of three other genes implicated in general cellular processes (*P. damicornis*: 60S ribosomal protein L22, 60S ribosomal protein L40A and 60S acidic ribosomal phosphoprotein P0; GenBank accession nos HO112261, HO112283 and HO112666, respectively) for comparison (Fig. 6Bi–iii).

Table 2. General characteristics of the BI, BR, TBI and TBR libraries

	BI	BR	TBI	TBR
Sequenced clone	384	384	384	384
Analysed cDNA	279	276	275	229
Mean EST size (bp)	335.9	332.1	367.3	302.7
Contigs	63	59	38	23
EST in contigs	156	127	91	63
Singletons	123	149	184	166
Redundancy* (%)	55.9	46.0	33.1	27.5

BI, bacteria-induced; BR, bacteria-repressed; EST, expressed sequence tag; TBI, thermo-bacteria-induced; TBR, thermo-bacteria-repressed.
*Redundancy=number of ESTs assembled in cluster/total EST.

To verify that all of the selected candidates (including the reference genes) were expressed by the coral cells rather than their symbionts, we performed cross-PCR experiments using DNA and cDNA extracted from the holobiont (host plus symbiont) and from pure cultured representatives of *Symbiodinium* spp. clades B, C and D (Fig. 7). The utilized primers included candidate-gene-specific oligonucleotides; primers ss5Z and ss3Z, which amplified the *Symbiodinium* spp. small ribosomal subunit (Rowan and Powers, 1991); and primers specific for the cDNA of the MBNP of *Symbiodinium* spp. The results revealed that the candidate genes could be amplified only from DNA and cDNA extracted from holobionts (Fig. 7), whereas the ss5Z/ss3Z and MBNP primers amplified all tested DNA and cDNA samples, respectively. This result shows that all of the selected candidate genes were specifically expressed by coral cells. In addition, results of this experiment for the genes encoding ferritin-like protein and the selenium-binding-protein-like protein show higher amplicon size when the matrix used was genomic DNA (Fig. 7). This is probably due to the presence of intronic sequences in both genes.

Two of the three selected lectins (concanavalin A-like protein and PdC-lectin) displayed similar transcriptional profiles (Fig. 6Ai,ii). Exposure to non-virulent bacteria triggered significant downregulation of concanavalin A-like protein and PdC-lectin at day 9 (more than fourfold and eightfold for PdC-lectin and concanavalin A-like protein, respectively), followed by upregulation at day 18 (only significant for PdC-lectin; 3.6-fold, $P<0.05$; Fig. 6Ai). In contrast, samples exposed to the virulent conditions showed significant upregulation of both genes from day 6 (2.9- and 3.3-fold for PdC-lectin and concanavalin A-like protein, respectively) to day 15, with a dramatic decrease seen on day 18. The maximum increase was observed on day 12 (7.7- and 9.3-fold for PdC-lectin and concanavalin A-like protein, respectively). The remaining lectin, P-selectin-like protein, differed from the other two; its expression decreased at all tested time points by more than 3.2-fold during the two experiments (Fig. 6Aiii).

The transcription patterns for ferritin-like protein and the selenium-binding-protein-like protein were very similar. In samples exposed to the non-virulent treatment, significant upregulation was observed across most of the tested time points (Fig. 6Aiv,v). In samples exposed to the virulent treatment, expression of ferritin-like protein was strongly downregulated at day 6 (10.2-fold), and then significantly upregulated at the end of the experiment (by more than 16.1-fold on day 18; Fig. 6Aiv). The gene encoding the selenium-binding-protein-like protein displayed a very similar profile (Fig. 6Av). Finally, cystatin B-like protein was downregulated

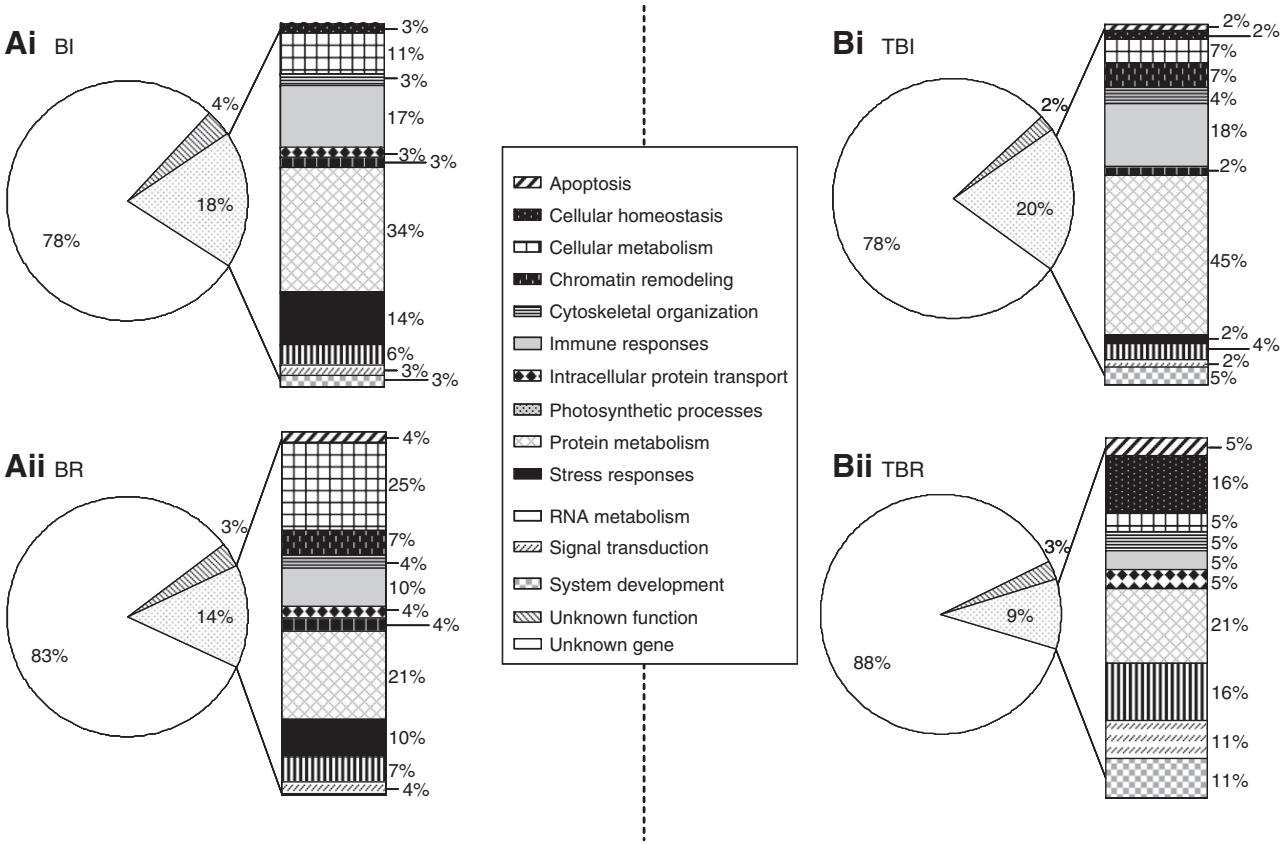

Fig. 5. Functional classification of the sequences obtained from the bacteria-induced (BI), bacteria-repressed (BR), thermo-bacteria-induced (TBI) and thermo-bacteria-repressed (TBR) libraries. Expressed sequence tags presenting similarities with genes of known function were clustered into 13 categories according to their putative biological functions. (A) Genes putatively upregulated (Ai) or downregulated (Aii) in *P. damicornis* exposed to *V. coralliilyticus* at a constant low temperature. (B) Genes putatively upregulated (Bi) or downregulated (Bii) in coral exposed to *V. coralliilyticus* under increasing seawater temperature (which triggers virulence).

at all tested time points in response to the non-virulent treatment (more than 3.1-fold; Fig. 6Avi), whereas under the virulent treatment it was significantly upregulated at day 15 and then downregulated at day 18 (more than 3.5-fold; Fig. 6Avi).

In our system, no significant expressional variation was observed among the general cellular process corresponding to reference genes (Fig. 6Bi–iii).

DISCUSSION

This work represents the first transcriptomic study investigating the physiological response of a scleractinian coral (*P. damicornis*) to its specific and temperature-sensitive pathogen, *V. coralliilyticus YB1*. More specifically, subtractive hybridization of mRNA from the holobiont subjected to balneation with bacteria at a constant (25°C) or increasing (25 to 32.5°C) temperature was used to identify immunity-related genes that appeared to be associated with bacterial stress or infection.

Although a previous study showed that bleaching was triggered by balneation of *P. damicornis* with *V. coralliilyticus YB1* at 25°C (Ben-Haim Rozenblat and Rosenberg, 2004), we surprisingly failed to observe bleaching under these conditions. However, this difference may be due to between-study differences in the utilized holobiont populations, which are known to display genetic variability (Pinzon and LaJeunesse, 2010). Eugene Rosenberg's group used an isolate of *P. damicornis* from Eilat in the Gulf of Aquaba (Red Sea, 29.30°N), where seawater temperatures range from 20.5 to 27.3°C (Ben-Haim Rozenblat and Rosenberg, 2004; Loya, 2004). In contrast, we used clones of an isolate of *P. damicornis* from Lombock Island (Indonesia, 8°S), where seawater temperatures range from 26.8 to 29.4°C (IGOSS: Integrated Global Ocean Services System; http://iridl.ldeo.columbia.edu/SOURCES/.IGOSS/). Thus these holobiont populations may have adapted to their local thermal conditions, as has been well documented in other species, including *Drosophila melanogaster*, *Podosphaera plantaginis*, *Scottolana canadensis*, *Daphnia magna* and various crustaceans (Lonsdale and Levinton, 1985; Whiteley et al., 1997; Mitchell and Lampert, 2000; Ayrinhac et al., 2004; Laine, 2008). In addition, differential responses under similar experimental conditions may arise through the actions of the mucus-associated bacterial community, as proposed in the hologenome theory of evolution (Rosenberg et al., 2007b). Although still under some debate, this theory contends that changes in the mucus-associated bacterial population can cause the coral holobiont to adapt to changes in the environment, including the presence of pathogens (Leggat et al., 2007; Rosenberg et al., 2007a; Rosenberg et al., 2007b).

In the context of temperature-dependent virulence, no lytic symptoms were observed at the low temperature (as expected). The first lytic events that could be observed by visual monitoring were noted on day 12 (29.5°C) in the Tb treatment. Microscopic analysis revealed that these visible lytic events were preceded by the development of bacterial aggregates inside ectodermal cells (first observed on day 9; Fig. 3A). In addition, the tissues surrounding

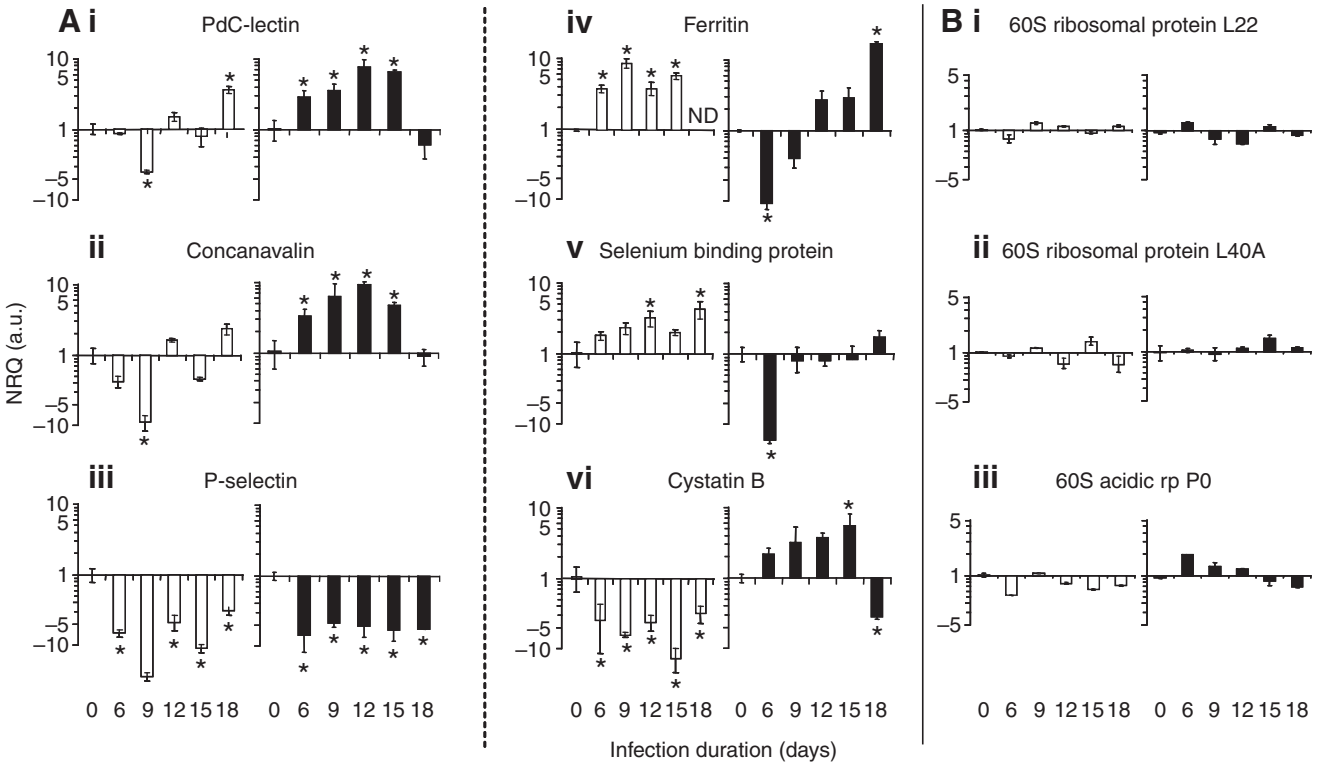

Fig. 6. Temporal expression patterns of selected candidate and reference genes. (A) qRT-PCR was used to measure the expression levels of six selected candidates from the non-virulent and virulent experiments on days 0, 6, 9, 12, 15 and 18. Relative expression levels were normalized with respect to the geometric mean of three reference genes (normalized relative quantity, NRQ). (B) Expression levels of the three reference genes normalized with respect to the expression of *P. damicornis* 28S rRNA. Open and filled histograms represent the results from the non-virulent and virulent experiments, respectively. Data are means ± s.e.m. of replicates. *, significant difference within the same group (P<0.05).

the bacteria aggregates were disorganized and the cellular organelles were mostly lysed (Fig. 3C). Similar aggregates were observed in a previous study by Ben-Haim et al. (Ben-Haim et al., 2003b), in which sections of *P. damicornis* infected by *V. coralliilyticus YB1* were analyzed using the same microscopic approach. Although *Vibrio* species are usually considered to be extracellular pathogens, several studies have reported intracellular and viable *Vibrio*. This was evidenced for another coral pathogen, *Vibrio shiloi*, invading *Oculina patagonica* epithelial cells (Banin et al., 2000), and for *Vibrio cholerae*, which can colonize amoebas (Abd et al., 2007) and phagocytes (Ma and Mekalanos, 2010). These results suggest that the applied temperature increase allowed infection by *V. coralliilyticus*, and that this infection was responsible for the lytic events leading to coral death.

To address the possibility that the detected aggregates could represent another bacterial species present in coral tissues, we quantified the amount of *V. coralliilyticus* in tissue samples from the Cb and Tb treatments at all time points. Our results revealed that the amount of *V. coralliilyticus* 16S rRNA in the *P. damicornis* tissues increased significantly by day 6 and remained high at the end of the experimental period. Collectively, these results suggest that *V. coralliilyticus* penetrates coral tissues, multiplies inside the ectodermal cells and triggers the lysis of organelles, cells and coral tissues.

In terms of transcriptomics, our SSH and EST analyses identified several interesting genes related to innate immunity as potentially being involved in the bacterial challenge. Six of them were chosen and used to monitor the response of coral to bacterial stress or infection.

Three of the chosen candidates corresponded to lectin-like molecules, which are known to play key roles in the pathogen-recognition processes of various invertebrates (Iwanaga and Lee, 2005; Schulenburg et al., 2008; Dunn, 2009). The first selected lectin-like molecule was similar to a mammalian P-selectin (Ley, 2003); the second displays similarities for concanavalin A-like (Rudenko et al., 1999; Grishkovskaya et al., 2000; Tisi et al., 2000; Buschiazzo et al., 2002); and the third, PdC-lectin, is likely to play a crucial role in the acquisition of zooxanthellae by coral cells (Vidal-Dupiol et al., 2009). Indeed, PdC-lectin is highly similar to another mannose binding lectin, the Millectin of *Acropora millepora*, which was shown to bind to both zooxanthellae and *V. coralliilyticus* (Kvennefors et al., 2008).

We found that the *PdC-lectin* and *concanavalin A-like* transcripts displayed similar expression patterns in non-virulent and virulent experiments. Their levels were upregulated in the virulent experiment from day 6 to 12, plateaued on day 15 (when the tank temperature reached 32.5°C) and then returned to the control level by day 18 (Fig. 6Ai,ii). This transcriptional induction is not surprising, as lectin-like genes have been found to be induced in a large set of studies on experimental infections of invertebrate species (O'Rourke et al., 2006; Huang et al., 2007; Gowda et al., 2008; Soonthornchai et al., 2010; Zhang et al., 2010). The day 18 decrease is more surprising, but many coral cells were undergoing necrosis at this stage (Fig. 1). Consequently, we can hypothesize that this day 18 decrease illustrates the physiological collapse of the coral,

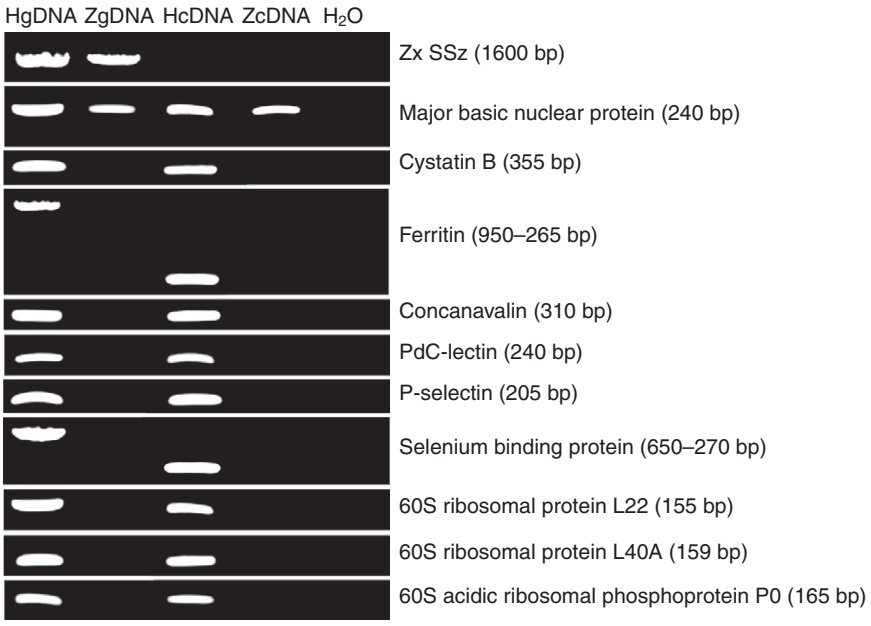

Fig. 7. The selected genes are expressed by the coral host. The presence of the selected candidate genes and those encoding the gene for the zooxanthellar small ribosomal subunit RNA (Zx SSz) and the cDNA of the zooxanthellar major basic nuclear protein were investigated by PCR amplification of DNA/cDNA extracted from holobionts (corals plus zooxanthellae) or from pools of pure cultured zooxanthellae representing clades B, C and D. HcDNA, holobiont cDNA; HgDNA, holobiont genomic DNA; ZcDNA, zooxanthellar cDNA; ZgDNA, zooxanthellar genomic DNA.

which could lead to a general decrease in the transcription levels of the genes responsible for a variety of functions. A general transcriptional decrease under extreme physiological conditions (lethal stress) has been observed previously in other species (Wang et al., 2006; Su et al., 2009).

In coral subjected to the non-virulent treatment, we observed a drastic transient decrease in the transcriptional expression levels of *PdC-lectin* and *concanavalin A-like protein* (Fig. 6Ai,ii). This transient decrease peaked on day 9 and the transcripts had returned to control levels by day 12. This observation is curious because no symptoms of infection were observed in this group. However, a similar downregulation of *PdC-lectin* was previously observed in *P. damicornis* nubbins confronted with thermal stress (Vidal-Dupiol et al., 2009), and occurred just prior to the dissociation of symbiosis and the onset of bleaching. Based on the putative role of PdC-lectin in the process of zooxanthellar acquisition, we previously hypothesized that this downregulation could lead to bleaching (Vidal-Dupiol et al., 2009). As corals have been reported to bleach under a wide variety of stress conditions, including high and low seawater temperature, increased heavy metal concentrations and decreased salinity (Brown, 1997; Douglas, 2003), we herein hypothesize that downregulation of *PdC-lectin* and *concanavalin A-like protein* could be induced by various stresses that lead to bleaching. The transient downregulation of these transcripts observed in the Cb treatment could be the result of stress induced by bacterial balneation. Although we did not observe any decrease in zooxanthellar density among these samples, it is possible that there may have been a temporary 'bleaching-like effect' without the appearance of visible symptoms. The further observation that the transcription levels of these genes returned to control levels allows us to hypothesize that the corals may have responded to the bacterial stress by reallocating their resources to prepare for an antibacterial response (e.g. the induction of ferritin expression; see below). Then, when the bacterial threat was gone, their allocations returned to 'business as usual'.

The third lectin, the *P-selectin–like protein*, was strongly downregulated after the initial addition of bacteria in both treatment groups, and this decrease was maintained for the duration of the experiments. The P-selectins have been well studied in vertebrate models, where they are known to be involved in various immune processes. However, their function in invertebrates is not yet known, making it somewhat difficult to interpret our present results. Interestingly, however, the P-selectins are known to be involved in adhesion processes (Rudenko et al., 1999; Grishkovskaya et al., 2000; Tisi et al., 2000; Buschiazzo et al., 2002), and studies have shown that some virulence factors present in the excretion–secretion products of marine *Vibrio* spp. reduced the adhesive properties of invertebrate hemocytes (Choquet et al., 2003; Allam and Ford, 2006; Labreuche et al., 2006a; Labreuche et al., 2006b; Mateo et al., 2009). Hemocyte-like cells have not yet been identified in scleractinians, but endodermal and circulating granular and agranular cells may have phagocytic properties (Mullen et al., 2004). Consequently, it may be useful in the future to explore the potential effect of *V. coralliilyticus* on the adhesive properties of *P. damicornis* phagocytes.

The three other candidates chosen to monitor the effect of *V. coralliilyticus* on the physiology of *P. damicornis* were *cystatin B-like*, *ferritin-like* and *selenium-binding-protein-like*. Cystatin B is a cytoplasmic protein that reversibly inhibits the cysteine proteases to affect protein turnover, and also plays a role in antibacterial defense (Zavasnik-Bergant, 2008). In vertebrates, *cystatin B* is upregulated in monocytes exposed to lipopolysaccharide challenge and treatment with immune enhancers (e.g. nitric oxide) (see Zavasnik-Bergant, 2008). In invertebrates, *cystatin B* is reportedly upregulated in response to bacterial challenge (Lefebvre et al., 2004) and parasitic infection (Kang et al., 2006). Our present results are in agreement with the previous findings, in that the transcriptional expression of the *cystatin B-like protein* increased when corals were infected by bacteria (virulent treatment). This induction peaked at day 15 and then sharply decreased by day 18. This drastic decrease could also be explained by the physiological collapse described above. Downregulation of *cystatin B-like protein* transcript levels was also observed in *P. damicornis* exposed to non-virulent bacteria, perhaps because of the existence of a trade-off mechanism allowing the coral to maximize its energy re-allocation to external defenses (i.e. the production of antibacterial compounds for release into the mucus). This phenomenon has been described for several invertebrate species in response to stress (Agell et al., 2004; Brulle et al., 2007; Lourenco et al., 2009).

The other putative immune effectors considered in the present study are two metal-binding proteins, a ferritin-like protein and a selenium-binding-protein-like protein. Ferritins, which can sequester iron, play dual roles in detoxification and iron storage (Arosio et al., 2009; Arosio and Levi, 2010), and the selenium-binding protein covalently binds selenium (Bansal et al., 1989; Jeong et al., 2009). Interestingly, iron appears to be essential for bacterial growth (Doherty, 2007), especially for *Vibrio* species (Wright et al., 1981; Tolmasky and Crosa, 1991; Wyckoff et al., 2007), and selenium is a trace element crucial for the survival of all living organisms through the formation of selenocysteine, a modified amino acid largely implicated in antioxidant defense (e.g. glutathione peroxidase, thioredoxin reductase) (Burk et al., 2003; Stadtman, 1996). Upregulation of ferritin and selenium-binding-protein by infected host cells can trigger iron and selenium sequestration, thereby reducing the amount of these essential trace elements necessary for bacterial growth. Infection-induced iron and selenium sequestration by ferritin and selenium-binding-protein have been observed in several other invertebrate–bacteria interactions (Beck et al., 2002; Song et al., 2006; Altincicek et al., 2008; Li et al., 2008; Kong et al., 2010; Simão et al., 2010), and the crucial role of ferritin in antibacterial defense was recently demonstrated in a study showing that the injection of recombinant ferritin into *Vibrio harveyi*-infected shrimp (*Peneaus monodon*) increased the host survival rate (Maiti et al., 2010).

Under non-virulent conditions, both *ferritin-like* and *selenium-binding-protein-like* were upregulated, perhaps reflecting that bacteria have been detected and the coral is preparing its defenses by sequestering iron and selenium. Under our virulent experimental conditions, the expression of *ferritin-like* and *selenium-binding-protein-like* corresponding genes was significantly downregulated during the early stage of infection, but upregulated near the end of the infection. This could illustrate that *V. coralliilyticus* is able to inhibit the intracellular immune response during the initial stages of infection. A similar phenomenon was observed in abalone following infection by *V. harveyi* (Travers et al., 2009). The upregulation of *ferritin-like* and *selenium-binding-protein-like* genes later in the process of infection could limit bacterial infection by sequestering iron and selenium. In addition, zooxanthellae under thermal stress have been shown to suffer photo-inhibition leading to ROS over-production (Weis, 2008). Thus, the overexpression of ferritin and selenium-binding-protein might also participate in ROS detoxification. Nevertheless, this late increase seems insufficient to overcome the *Vibrio* infection process, at least under our experimental conditions.

In conclusion, the present study represents the first molecular examination of the response evoked by a scleractinian coral when confronted by its pathogenic *Vibrio* (*V. coralliilyticus*). Several genes that appeared to be involved in the coral immune response were identified, and their expression patterns were studied in corals exposed to virulent and non-virulent bacteria. The results revealed clear differences for some of the candidate genes, which could prove useful as functional biomarkers for measuring coral health and immunity in monitoring programs and public aquariums. Future studies will be required to fully examine the molecular and cellular mechanisms involved in this process, but our study also suggests several new hypotheses concerning the effect of *V. coralliilyticus* on the physiology of *P. damicornis*.

ACKNOWLEDGEMENTS

This work was supported by the Centre National pour la Recherche Scientifique (CNRS). O.L. is a PhD student of the National Fund for Scientific Research (FNRS-Fonds National de la Recherche Scientifique, Belgium). The authors are indebted to Marc Manetti for his help with the experimental procedures, Céline Cosseau for many helpful discussions and Andrew Carroll for English proofreading and helpful discussions. We thank Alain Pigno and Boris Rota from the Cap d'Agde Public Aquarium for their help with the project, and Jérôme Bossier for helping with the statistical analyses. We also thank the Department of Environmental Sciences and Management (Prof. J. P. Thome) and the Dean of the Faculty of Sciences (Prof. J. M. Bouquegneau), both of the University of Liege, for financial support. Finally, the authors thank Mary-Alice Coffroth for allowing us to use cultures from the BURR Culture Collection.

REFERENCES

Abd, H., Saeed, A., Weintraub, A., Nair, G. B. and Sandström, G. (2007). *Vibrio cholerae* O1 strains are facultative intracellular bacteria, able to survive and multiply symbiotically inside the aquatic free-living amoeba *Acanthamoeba castellanii*. *FEMS Microbiol. Ecol.* **60**, 33-39.

Agell, G., Turon, X., De Caralt, S., López-Legentil, S. and Uriz, M. J. (2004). Molecular and organism biomarkers of copper pollution in the ascidian *Pseudodistoma crucigaster*. *Mar. Pollut. Bull.* **48**, 759-767.

Allam, B. and Ford, S. E. (2006). Effects of the pathogenic *Vibrio tapetis* on defence factors of susceptible and non-susceptible bivalve species: I. Haemocyte changes following in vitro challenge. *Fish Shellfish Immunol.* **20**, 374-383.

Altincicek, B., Knorr, E. and Vilcinskas, A. (2008). Beetle immunity: identification of immune-inducible genes from the model insect *Tribolium castaneum*. *Dev. Comp. Immunol.* **32**, 585-595.

Arosio, P. and Levi, S. (2010). Cytosolic and mitochondrial ferritins in the regulation of cellular iron homeostasis and oxidative damage. *Biochim. Biophys. Acta* **1800**, 783-792.

Arosio, P., Ingrassia, R. and Cavadini, P. (2009). Ferritins: a family of molecules for iron storage, antioxidation and more. *Biochim. Biophys. Acta* **1790**, 589-599.

Ayrinhac, A., Debat, V., Gibert, P., Kister, A.-G., Legout, H., Moreteau, B., Vergilino, R. and David, J. R. (2004). Cold adaptation in geographical populations of *Drosophila melanogaster*: phenotypic plasticity is more important than genetic variability. *Funct. Ecol.* **18**, 700-706.

Banin, E., Israely, T., Kushmaro, A., Loya, Y., Orr, E. and Rosenberg, E. (2000). Penetration of the coral-bleaching bacterium *Vibrio shiloi* into *Oculina patagonica*. *Appl. Environ. Microbiol.* **66**, 3031-3036.

Banin, E., Sanjay, K. H., Naider, F. and Rosenberg, E. (2001). A proline rich peptide from the coral pathogen *Vibrio shiloi* that inhibits photosynthesis of zooxanthellae. *Appl. Environ. Microbiol.* **67**, 1536-1541.

Bansal, M. P., Oborn, C. J., Danielson, K. G. and Medina, D. (1989). Evidence for two selenium-binding proteins distinct from glutathione peroxidase in mouse liver. *Carcinogenesis* **10**, 541-546.

Beck, G., Ellis, T. W., Habicht, G. S., Schluter, S. F. and Marchalonis, J. J. (2002). Evolution of the acute phase response: iron release by echinoderm (*Asterias forbesi*) coelomocytes, and cloning of an echinoderm ferritin molecule. *Dev. Comp. Immunol.* **26**, 11-26.

Ben-Haim, Y. and Rosenberg, E. (2002). A novel *Vibrio* sp. pathogen of the coral *Pocillopora damicornis*. *Mar. Biol.* **141**, 47-55.

Ben-Haim, Y., Thompson, F. L., Thompson, C. C., Cnockaert, M. C., Hoste, B., Swings, J. and Rosenberg, E. (2003a). *Vibrio coralliilyticus* sp. nov., a temperature-dependent pathogen of the coral *Pocillopora damicornis*. *Int. J. Syst. Evol. Microbiol.* **53**, 309-315.

Ben-Haim, Y., Zicherman-Keren, M. and Rosenberg, E. (2003b). Temperature-regulated bleaching and lysis of the coral *Pocillopora damicornis* by the novel pathogen *Vibrio coralliilyticus*. *Appl. Environ. Microbiol.* **69**, 4236-4242.

Ben-Haim Rozenblat, Y. and Rosenberg, E. (2004). Temperature-regulated bleaching and tissue lysis of *Pocillopora damicornis* by the novel pathogen *Vibrio coralliilyticus*. In *Coral Health and Disease* (ed. E. Rosenberg and Y. Loya), pp. 301-324. New-York: Spinger-Verlag.

Bourne, D. G., Garren, M., Work, T. M., Rosenberg, E., Smith, G. W. and Harvell, C. D. (2009). Microbial disease and the coral holobiont. *Trends Microbiol.* **17**, 554-562.

Brown, B. E. (1997). Coral bleaching: causes and consequences. *Coral Reefs* **16**, S129-S138.

Brulle, F., Mitta, G., Leroux, R., Lemière, S., Leprêtre, A. and Vandenbulcke, F. (2007). The strong induction of metallothionein gene following cadmium exposure transiently affects the expression of many genes in *Eisenia fetida*: a trade-off mechanism? *Comp. Biochem. Physiol.* **144C**, 334-341.

Burk, R. F., Hill, K. E. and Motley, A. K. (2003). Selenoprotein metabolism and function: evidence for more than one function for selenoprotein P. *J. Nutr.* **133**, 1517-1520.

Buschiazzo, A., Amaya, M. F., Cremona, M. L., Frasch, A. C. and Alzari, P. M. (2002). The crystal structure and mode of action of trans-sialidase, a key enzyme in *Trypanosoma cruzi* pathogenesis. *Mol. Cell* **10**, 757-768.

Cervino, J. M., Hayes, R. L., Polson, S. W., Polson, S. C., Goreau, T. J., Martinez, R. J. and Smith, G. W. (2004). Relationship of *Vibrio* species infection and elevated temperatures to yellow blotch/band disease in Caribbean corals. *Appl. Environ. Microbiol.* **70**, 6855-6864.

Cervino, J. M., Thompson, F. L., Gomez-Gil, B., Lorence, E. A., Goreau, T. J., Hayes, M. L., Winiarski-Cervino, K. B., Smith, D. J., Hughen, K. and Bartels, E. (2008). The *Vibrio* core group induces yellow band disease in Caribbean and Indo-Pacific reef-building corals. *J. Appl. Microbiol.* **105**, 1658-1671.

Choquet, G., Soudant, P., Lambert, C., Nicolas, J.-L. and Paillard, C. (2003). Reduction of adhesion properties of *Ruditapes philippinarum* hemocytes exposed to *Vibrio tapetis*. *Dis. Aquat. Org.* **57**, 109-116.

Doherty, C. P. (2007). Host-pathogen interactions: the role of iron. *J. Nutr.* **137**, 1341-1344.

Donner, S. D., Skirving, W. J., Little, C. M., Oppenheimer, M. and Hoegh-Guldberg, O. V. E. (2005). Global assessment of coral bleaching and required rates of adaptation under climate change. *Glob. Change Biol.* **11**, 2251-2265.
Douglas, A. E. (2003). Coral bleaching-how and why? *Mar. Pollut. Bull.* **46**, 385-392.
Dunn, S. R. (2009). Immunorecognition and immunoreceptors in the Cnidaria. *Invertebrate Surviv. J.* **6**, 7-14.
Gates, R. D., Baghdasarian, G. and Muscatine, L. (1992). Temperature stress caused host cell detachent in symbiotic cnidarians: implications for coral bleaching. *Biol. Bull.* **182**, 324-332.
Gowda, N. M., Goswami, U. and Islam Khan, M. (2008). T-antigen binding lectin with antibacterial activity from marine invertebrate, sea cucumber (*Holothuria scabra*): possible involvement in differential recognition of bacteria. *J. Invertebr. Pathol.* **99**, 141-145.
Grishkovskaya, I., Avvakumov, G. V., Sklenar, G., Dales, D., Hammond, G. L. and Muller, Y. A. (2000). Crystal structure of human sex hormone-binding globulin: steroid transport by a laminin G-like domain. *EMBO J.* **19**, 504-512.
Grubbs, F. E. (1969). Procedures for detecting outlying observations in samples. *Technometrics* **11**, 1-21.
Harvell, D., Jordán-Dahlgren, E., Merkel, S., Rosenberg, E., Raymundo, L., Smith, G., Weil, E. and Willis, B. (2007). Coral disease, environmental drivers, and the balance between coral and microbial associates. *Oceanography* **20**, 172-195.
Hashimoto, K., Shibuno, T., Murayama-Kayano, E., Tanaka, H. and Kayano, T. (2004). Isolation and characterization of stress-responsive genes from the scleractinian coral *Pocillopora damicornis*. *Coral Reefs* **23**, 485-491.
Hellemans, J., Mortier, G., De Paepe, A., Speleman, F. and Vandesompele, J. (2007). qBase relative quantification framework and software for management and automated analysis of real-time quantitative PCR data. *Genome Biol.* **8**, R19.
Hoegh-Guldberg, O., Mumby, P. J., Hooten, A. J., Steneck, R. S., Greenfield, P., Gomez, E., Harvell, C. D., Sale, P. F., Edwards, A. J., Caldeira, K. et al. (2007). Coral reefs under rapid climate change and ocean acidification. *Science* **318**, 1737-1742.
Huang, G., Liu, H., Han, Y., Fan, L., Zhang, Q., Liu, J., Yu, X., Zhang, L., Chen, S., Dong, M. et al. (2007). Profile of acute immune response in Chinese amphioxus upon *Staphylococcus aureus* and *Vibrio parahaemolyticus* infection. *Dev. Comp. Immunol.* **31**, 1013-1023.
Hughes, T., Baird, A., Bellwood, D., Card, M., Connolly, S., Folke, C., Grosberg, R., Guldberg, H., Jackson, J., Kleypas, J. et al. (2003). Climate change, human impacts, and the resilience of coral reefs. *Science* **301**, 929-933.
Iwanaga, S. and Lee, B. R. (2005). Recent advances in the innate immunity of invertebrate animals. *J. Biochem. Mol. Biol.* **38**, 128-150.
Jeong, J.-Y., Wang, Y. and Sytkowski, A. J. (2009). Human selenium binding protein-1 (hSP56) interacts with VDU1 in a selenium-dependent manner. *Biochem. Biophys. Res. Commun.* **379**, 583-588.
Johannes, R. E. and Wiebe, W. J. (1970). Method for determination of coral tissue biomass and composition. *Limnol. Oceanogr.* **15**, 822-824.
Kang, Y.-S., Kim, Y.-M., Park, K.-I., Kim Cho, S., Choi, K.-S. and Cho, M. (2006). Analysis of EST and lectin expressions in hemocytes of Manila clams (*Ruditapes philippinarum*) (Bivalvia: Mollusca) infected with *Perkinsus olseni*. *Dev. Comp. Immunol.* **30**, 1119-1131.
Kong, P., Wang, L., Zhang, H., Zhou, Z., Qiu, L., Gai, Y. and Song, L. (2010). Two novel secreted ferritins involved in immune defense of Chinese mitten crab *Eriocheir sinensis*. *Fish Shellfish Immunol.* **28**, 604-612.
Kushmaro, A., Loya, Y., Fine, M. and Rosenberg, E. (1996). Bacterial infection and bleaching. *Nature* **380**, 396.
Kushmaro, A., Rosenberg, E., Fine, M. and Loya, Y. (1997). Bleaching of the coral *Oculina patagonica* by *Vibrio AK-1*. *Mar. Ecol. Prog. Ser.* **147**, 159-165.
Kushmaro, A., Rosenberg, E., Fine, M., Ben Haim, H. and Loya, Y. (1998). Effect of temperature on bleaching of the coral *Oculina patagonica* by *Vibrio* AK-1. *Mar. Ecol. Prog. Ser.* **171**, 131-137.
Kushmaro, A., Banin, E., Loya, Y., Stackebrandt, E. and Rosenberg, E. (2001). *Vibrio shiloi* sp. nov., the causative agent of bleaching of the coral *Oculina patagonica*. *Int. J. Syst. Evol. Microbiol.* **51**, 1383-1388.
Kvennefors, E. C. E., Leggat, W., Hoegh-Guldberg, O., Degnan, B. M. and Barnes, A. C. (2008). An ancient and variable mannose-binding lectin from the coral *Acropora millepora* binds both pathogens and symbionts. *Dev. Comp. Immunol.* **32**, 1582-1592.
Labreuche, Y., Lambert, C., Soudant, P., Boulo, V., Huvet, A. and Nicolas, J.-L. (2006a). Cellular and molecular hemocyte responses of the Pacific oyster, *Crassostrea gigas*, following bacterial infection with *Vibrio aestuarianus* strain 01/32. *Microbes Infect.* **8**, 2715-2724.
Labreuche, Y., Soudant, P., Gonçalves, M., Lambert, C. and Nicolas, J.-L. (2006b). Effects of extracellular products from the pathogenic *Vibrio aestuarianus* strain 01/32 on lethality and cellular immune responses of the oyster *Crassostrea gigas*. *Dev. Comp. Immunol.* **30**, 367-379.
Ladrière, O., Compère, P., Decloux, N., Vandewalle, P. and Poulicek, M. (2008). Morphological alterations of zooxanthellae in bleached cnidarian hosts. *Cahiers Biol. Mar.* **49**, 215-227.
Laine, A.-L. (2008). Temperature-mediated patterns of local adaptation in a natural plant pathogen metapopulation. *Ecol. Lett.* **11**, 327-337.
Lefebvre, C., Cocquerelle, C., Vandenbulcke, F., Hot, D., Huot, L., Lemoine, Y. and Salzet, M. (2004). Transcriptomic analysis in the leech *Theromyzon tessulatum*: involvement of cystatin B in innate immunity. *Biochem. J.* **380**, 617-625.
Leggat, W., Ainsworth, T., Bythell, J., Dove, S., Gates, R., Hoegh-Guldberg, O., Iglesias-Prieto, R. and Yellowlees, D. (2007). The hologenome theory disregards the coral holobiont. *Nat. Rev. Microbiol.* **5**. doi:10.1038/nrmicro1635-c1
Lesser, M. P. (2004). Experimental biology of coral reef ecosystems. *J. Exp. Mar. Biol. Ecol.* **300**, 217-252.
Ley, K. (2003). The role of selectins in inflammation and disease. *Trends Mol. Med.* **9**, 263-268.
Li, M., Saren, G. and Zhang, S. (2008). Identification and expression of a ferritin homolog in amphioxus *Branchiostoma belcheri*: evidence for its dual role in immune response and iron metabolism. *Comp. Biochem. Physiol.* **150B**, 263-270.
Lonsdale, D. J. and Levinton, J. S. (1985). Latitudinal differentiation in copepod growth: an adaptation to temperature. *Ecology* **66**, 1397-1407.
Lourenco, A. P., Martins, J. R., Bitondi, M. M. G. and Simoes, Z. L. P. (2009). Trade-off between immune stimulation and expression of storage protein genes *Arch. Insect Biochem. Physiol.* **71**, 70-87.
Loya, Y. (2004). The coral reefs of Eilat-past, present and future: three decades of coral comunity structure studies. In *Coral Health and Disease* (ed. E. Rosenberg and Y. Loya), pp. 1-29. Berlin, Heidelberg: Spinger-Verlag.
Luna, G. M., Biavasco, F. and Danovaro, R. (2007). Bacteria associated with the rapid tissue necrosis of stony corals. *Environ. Microbiol.* **9**, 1851-1857.
Ma, A. T. and Mekalanos, J. J. (2010). In vivo actin cross-linking induced by *Vibrio cholerae* type VI secretion system is associated with intestinal inflammation. *Proc. Natl. Acad. Sci. USA* **107**, 4365-4370.
Maiti, B., Khushiramani, R., Tyagi, A., Karunasagar, I. and Karunasagar, I. (2010). Recombinant ferritin protein protects *Penaeus monodon* infected by pathogenic *Vibrio harveyi*. *Dis. Aquat. Org.* **88**, 99-105.
Mateo, D. R., Siah, A., Araya, M. T., Berthe, F. C. J., Johnson, G. R. and Greenwood, S. J. (2009). Differential in vivo response of soft-shell clam hemocytes against two strains of *Vibrio splendidus*: changes in cell structure, numbers and adherence. *J. Invertebr. Pathol.* **102**, 50-56.
Mitchell, S. E. and Lampert, W. (2000). Temperature adaptation in a geographically widespread zooplankter, *Daphnia magna*. *J. Evol. Biol.* **13**, 371-382.
Mullen, K. M., Peters, E. C. and Harvell, C. D. (2004). Coral resistance to disease. In *Coral Health and Disease* (ed. E. Rosenberg and Y. Loya), pp. 377-399. Berlin, Heidelberg: Spinger-Verlag.
O'Rourke, D., Baban, D., Demidova, M., Mott, R. and Hodgkin, J. (2006). Genomic clusters, putative pathogen recognition molecules, and antimicrobial genes are induced by infection of *C. elegans* with *M. nematophilum*. *Genome Res.* **16**, 1005-1016.
Pinzon, H. and LaJeunesse, T. C. (2010). Species delimitation of common reef corals in the genus *Pocillopora* using nucleotide sequence phylogenies, population genetics and symbiosis ecology. *Mol. Ecol.* **20**, 311-325.
Putnam, N. H., Srivastava, M., Hellsten, U., Dirks, B., Chapman, J., Salamov, A., Terry, A., Shapiro, H., Lindquist, E., Kapitonov, V. V. et al. (2007). Sea anemone genome reveals ancestral eumetazoan gene repertoire and genomic organization. *Science* **317**, 86-94.
Putnam, N. H., Butts, T., Ferrier, D. E. K., Furlong, R. F., Hellsten, U., Kawashima, T., Robinson-Rechavi, M., Shoguchi, E., Terry, A., Yu, J.-K. et al. (2008). The amphioxus genome and the evolution of the chordate karyotype. *Nature* **453**, 1064-1071.
Rodriguez-Lanetty, M., Harii, S. and Hoegh-Guldberg, O. (2009). Early molecular responses of coral larvae to hyperthermal stress. *Mol. Ecol.* **18**, 5101-5114.
Rosenberg, E. (2004). The bacterial disease hypothesis of coral bleaching. In *Coral Health and Disease* (ed. E. Rosenberg and Y. Loya), pp. 377-399. Berlin, Heidelberg: Spinger-Verlag.
Rosenberg, E., Koren, O., Reshef, L., Efrony, R. and Zilber-Rosenberg, I. (2007a). The hologenome theory disregards the coral holobiont: reply from Rosenberg et al. *Nat. Rev. Microbiol.* **5**, doi:10.1038/nrmicro1635-c2
Rosenberg, E., Koren, O., Reshef, L., Efrony, R. and Zilber-Rosenberg, I. (2007b). The role of microorganisms in coral health, disease and evolution. *Nat. Rev. Microbiol.* **5**, 355-362.
Rowan, R. and Powers, D. A. (1991). Molecular genetic identification of symbiotics dinoflagellates (zooxanthellae). *Mar. Ecol. Prog. Ser.* **71**, 65-73.
Rudenko, G., Nguyen, T., Chelliah, Y., Südhof, T. C. and Deisenhofer, J. (1999). Regulation of LNS domain function by alternative splicing: the structure of the ligand-binding domain of Neurexin I β. *Cell* **99**, 93-101.
Schulenburg, H., Hoeppner, M. P., Weiner, J. R. and Bornberg-Bauer, E. (2008). Specificity of the innate immune system and diversity of C-type lectin domain (CTLD) proteins in the nematode *Caenorhabditis elegans*. *Immunobiology* **213**, 237-250.
Simão, M., Leite, R., Rocha, C. and Cancela, M. (2010). Changes in bioturbation of iron biogeochemistry and in molecular response of the clam *Ruditapes decussates* upon *Perkinsus olseni* infection. *Arch. Environ. Contam. Toxicol.* **59**, 433-443.
Song, L., Zou, H., Chang, Y., Xu, W. and Wu, L. (2006). The cDNA cloning and mRNA expression of a potential selenium-binding protein gene in the scallop *Chlamys farreri*. *Dev. Comp. Immunol.* **30**, 265-273.
Soonthornchai, W., Rungrassamee, W., Karoonuthaisiri, N., Jarayabhand, P., Klinbunga, S., Söderhäll, K. and Jiravanichpaisal, P. (2010). Expression of immune-related genes in the digestive organ of shrimp, *Penaeus monodon*, after an oral infection by *Vibrio harveyi*. *Dev. Comp. Immunol.* **34**, 19-28.
Stadtman, T. C. (1996). Selenocysteine. *Annu. Rev. Biochem.* **65**, 83-100.
Stefansky, W. (1972). Rejecting outliers in factorial designs. *Technometrics* **14**, 469-479.
Stimson, J. and Kinzie, R. A., III (1991). The temporal pattern and rate of release of zooxanthellae from the reef coral *Pocillopora damicornis* (Linnaeus) under nitrogen-enrichment and control conditions. *J. Exp. Mar. Biol. Ecol.* **153**, 63-74.
Stimson, J., Sakai, K. and Sembali, H. (2002). Interspecific comparison of the symbiotic relationship in corals with high and low rates of bleaching-induced mortality. *Coral Reefs* **21**, 409-421.
Su, J., Yang, C., Xiong, F., Wang, Y. and Zhu, Z. (2009). Toll-like receptor 4 signaling pathway can be triggered by grass carp reovirus and *Aeromonas hydrophila* infection in rare minnow *Gobiocypris rarus*. *Fish Shellfish Immunol.* **27**, 33-39.
Sussman, M., Willis, B. L., Victor, S. and Bourne, D. G. (2008). Coral pathogens identified for white syndrome (WS) epizootics in the Indo-Pacific. *Plos ONE* **3**, e2393.
Sutherland, K. P., Porter, J. W. and Torres, C. (2004). Disease and immunity in Caribbean and Indo-Pacific zooxanthellate corals. *Mar. Ecol. Prog. Ser.* **266**, 273-302.

Tisi, D., Talts, J. F., Timpl, R. and Hohenester, E. (2000). Structure of the C-terminal laminin G-like domain pair of the laminin α2 chain harbouring binding sites for α-dystroglycan and heparin. *EMBO J.* **19**, 1432-1440.
Tolmasky, M. E. and Crosa, J. H. (1991). Regulation of plasmid-mediated iron transport and virulence in *Vibrio anguillarum*. *Biometals* **4**, 33-35.
Travers, M. A., Le Bouffant, R., Friedman, C. S., Buzin, F., Cougard, B., Huchette, S., Koken, M. and Paillard, C. (2009). Pathogenic *Vibrio harveyi* in contrast to non-pathogenic strains, intervenes with the p38 MAPK pathway to avoid an abalone haemocyte immune response. *J. Cell. Biochem.* **106**, 152-160.
Veron, J. E. N. (2000). *Corals of the World*. Townsville, Australia: Australian Institute of Marine Science.
Vidal-Dupiol, J., Adjeroud, M., Roger, E., Foure, L., Duval, D., Mone, Y., Ferrier-Pages, C., Tambutte, E., Tambutte, S., Zoccola, D. et al. (2009). Coral bleaching under thermal stress: putative involvement of host/symbiont recognition mechanisms. *BMC Physiol.* **9**, 14.
Wang, B., Li, F., Dong, B., Zhang, X., Zhang, C. and Xiang, J. (2006). Discovery of the genes in response to White Spot Syndrome Virus (WSSV) infection in *Fenneropenaeus chinensis* through cDNA microarray. *Mar. Biotechnol.* **8**, 491-500.
Ward, J. R. and Lafferty, K. D. (2004). The elusive baseline of marine disease: are diseases in ocean ecosystems increasing? *PLoS Biol.* **2**, e120.
Ward, J. R., Kim, K. and Harvell, C. D. (2007). Temperature affects coral disease resistance and pathogen growth. *Mar. Ecol. Prog. Ser.* **329**, 115-121.
Weil, E., Smith, G. W. and Gil-Agudelo, D. L. (2006). Status and progress in coral reef disease research. *Dis. Aquat. Org.* **69**, 1-7.
Weis, V. M. (2008). Cellular mechanisms of Cnidarian bleaching: stress causes the collapse of symbiosis. *J. Exp. Biol.* **211**, 3059-3066.
Whiteley, N. M., Taylor, E. W. and El Haj, A. J. (1997). Seasonal and latitudinal adaptation to temperature in crustaceans. *J. Therm. Biol.* **22**, 419-427.
Wilkinson, C. (ed.) (2008). *Status of Coral Reefs of the World*, 296 pp. Townsville, Australia: Global Coral Reef Monitoring Network and Reef and Rainforest Research Center.
Willis, B. L., Page, C. A. and Dinsdale, E. A. (2004). Coral diseases on the great barrier reef. In *Coral Health and Disease* (ed. E. Rosenberg and Y. Loya), pp. 69-104. New York: Springer-Verlag.
Wright, A. C., Simpson, L. M. and Oliver, J. D. (1981). Role of iron in the pathogenesis of *Vibrio vulnificus* infections. *Infect. Immun.* **34**, 503-507.
Wyckoff, E., Mey, A. and Payne, S. (2007). Iron acquisition in *Vibrio cholerae*. *Biometals* **20**, 405-416.
Yuan, J. S., Reed, A., Chen, F. and Stewart, C. N., Jr (2006). Statistical analysis of real-time PCR data. *BMC Bioinformatics* **7**, 85-97.
Zavasnik-Bergant, T. (2008). Cystatin protease inhibitors and immune functions. *Front. Biosci.* **13**, 4625-4637.
Zhang, H., Kong, P., Wang, L., Zhou, Z., Yang, J., Zhang, Y., Qiu, L. and Song, L. (2010). Cflec-5, a pattern recognition receptor in scallop *Chlamys farreri* agglutinating yeast *Pichia pastoris*. *Fish Shellfish Immunol.* **29**, 149-156.

Table S1. Cluster number, annotation, top BLASTX, top BLAST with functional similarity, functional classification and GenBank accession numbers of the annotated expressed sequence tags for the BI, BR, TBI and TBR libraries

Library cluster no.	Annotation	Top BLASTX protein [species]	*E*	Top BLAST functional similarity protein [species]	*E*	Functional classification	GenBank accession no.
B-I-146	Putative spore formation protein K	spore formation protein K [Bacillus clausii KSM-K16]	8.10^{-20}			Cellular metabolic process	HO112242
B-I-147	Actin	actin [Stylophora pistillata]	3.10^{-74}			Cytoskeleton organization	HO112243
B-I-148	Arylsulfatase	predicted protein [Nematostella vectensis]	1.10^{-12}	similar to arylsulfatase J [Gallus gallus]	1.10^{-9}	Cellular metabolic process	HO112244
B-I-149	ATP-dependent RNA helicase, eIF4A related	ATP-dependent RNA helicase, eIF4A related [Schizosaccharomyces pombe 972h-]	6.10^{-4}			RNA metabolic process	HO112245
B-I-150	Carbonic anhydrase	carbonic anhydrase [Desulfovibrio vulgaris str. 'Miyazaki F']	2.10^{-4}			Response to stress	HO112247
B-I-151	CCAAT/Enhancer binding protein beta	predicted protein [Nematostella vectensis]	6.10^{-20}	CCAAT/Enhancer binding protein beta [Paralichthys olivaceus]	1.10^{-19}	Immune response	HO112248
B-I-153	DEAH (Asp-Glu-Ala-His) box polypeptide 15	DEAH (Asp-Glu-Ala-His) box polypeptide 15 [Hydra magnipapillata]	4.10^{-4}			Response to stress	HO112250
B-I-156	Proline-rich transmembrane protein 1	hypothetical protein BRAFLDRAFT_74660 [Branchiostoma floridae]	7.10^{-14}	proline-rich transmembrane protein 1 [Porphyromonas endodontalis ATCC 35406]	5.10^{-7}	Immune response	HO112253
B-I-159	Epsilon subunit of ATP synthetase	hypothetical protein [Strongylocentrotus purpuratus]	4.10^{-8}	epsilon subunit of ATP synthetase [Hydroides elegans]	2.10^{-6}	Cellular metabolic process	HO112256
B-I-160	Putative lysyl-tRNA synthetase	lysyl-tRNA synthetase, putative [Perkinsus marinus ATCC 50983]	7.10^{-19}			Protein metabolic process	HO112258
B-I-161	Antho-RFamide neuropeptides	Antho-RFamide Precursor [Calliactis parasitica]	6.10^{-41}			Signal transduction	HO112259
B-I-162	NOD3 protein	predicted protein [Nematostella vectensis]	2.10^{-30}	NOD3 protein, isoform CRA_d [Homo sapiens]	1.10^{-29}	Immune response	HO112260
B-I-163	60S ribosomal protein L22	predicted protein [Nematostella vectensis]	9.10^{-24}	60S ribosomal protein L22, putative [Pediculus humanus corporis]	3.10^{-21}	Protein metabolic process	HO112261
B-I-164	60S ribosomal protein, Rpl7A	predicted protein [Nematostella vectensis]	2.10^{-25}	60S ribosomal protein, Rpl7A [Seculamonas ecuadoriensis]	1.10^{-24}	Protein metabolic process	HO112262
B-I-165	Ribosomal protein S10	predicted protein [Nematostella vectensis]	2.10^{-17}	ribosomal protein S10 [Crassostrea gigas]	1.10^{-8}	Protein metabolic process	HO112263
B-I-166	Ribosomal protein S19	predicted protein [Nematostella vectensis]	1.10^{-15}	ribosomal protein S19, isoform CRA_b [Homo sapiens]	3.10^{-14}	Protein metabolic process	HO112264
B-I-167	Similar to Zinc finger RNA-binding protein	similar to Zinc finger RNA-binding protein [Bos taurus]	1.10^{-7}			RNA metabolic process	HO112265
B-I-168	Peridinin chlorophyll-a binding protein apoprotein precursor	peridinin chlorophyll-a binding protein apoprotein precursor [Symbiodinium kawagutii]	1.10^{-15}			Photosynthetic process	HO112266
B-I-169	Peroxiredoxin 6	predicted protein [Nematostella vectensis]	1.10^{-43}	peroxiredoxin 6 [Haliotis discus discus]	1.10^{-41}	Response to stress	HO112267
B-I-170	Symbiot Polyubiquitin	polyubiquitin [Symbiodinium sp. C3]	7.10^{-24}			Protein metabolic process	HO112269
B-I-172	similar to Solute carrier family 30	predicted protein [Nematostella vectensis]	5.10^{-20}	similar to Solute carrier family 30 (zinc transporter), member 5 [Strongylocentrotus purpuratus]	6.10^{-11}	Cellular homeostasis	HO112271
B-I-173	Ornithine decarboxylase antizyme 2	predicted protein [Nematostella vectensis]	2.10^{-14}	ornithine decarboxylase antizyme 2 [Danio rerio]	2.10^{-8}	Cellular metabolic process	HO112272
B-I-174	Peptidyl-dipeptidase A	predicted protein [Nematostella vectensis]	2.10^{-9}	peptidyl-dipeptidase A [Acidobacteria bacterium Ellin345]	7.10^{-8}	Response to stress	HO112273

B-I-175	Similar to placenta-specific 8	predicted protein [Nematostella vectensis]	1.10^{-20}	PREDICTED: similar to placenta-specific 8 [Ciona intestinalis]	8.10^{-7}	Immune response	HO112274
B-I-176	Putative Sec61 protein translocation complex beta-subunit	hypothetical protein BRAFLDRAFT_284448 [Branchiostoma floridae]	1.10^{-12}	Sec61 protein translocation complex beta-subunit, putative [Ixodes scapularis]	1.10^{-10}	Intracellular protein transport	HO112275
B-I-177	Similar to Pema-SRCR protein	predicted protein [Nematostella vectensis]	1.10^{-6}	PREDICTED: similar to Pema-SRCR protein [Strongylocentrotus purpuratus]	5.10^{-5}	Immune response	HO112276
B-I-181	Similar to 40S ribosomal protein S2	PREDICTED: similar to 40S ribosomal protein S2 [Gallus gallus]	7.10^{-24}			Protein metabolic process	HO112281
B-I-182	Ribosomal protein L11	ribosomal protein L11 [Lysiphlebus testaceipes]	5.10^{-78}			Protein metabolic process	HO112282
B-I-183	60S ribosomal protein L40A	60S ribosomal protein L40A [Lycosa singoriensis]	4.10^{-21}			Protein metabolic process	HO112283
B-I-184	Ribosomal protein rps12	ribosomal protein rps12 [Eurythoe complanata]	3.10^{-61}			Protein metabolic process	HO112284
B-I-185	Putative 60S ribosomal protein RPL10	predicted protein [Nematostella vectensis]	5.10^{-103}	putative 60S ribosomal protein RPL10 [Phoronis muelleri]	1.10^{-98}	Protein metabolic process	HO112285
B-I-186	Serotransferrin	serotransferrin [Gillichthys mirabilis]	1.10^{-4}			System development	HO112286
B-I-188	small heat shock protein	small heat shock protein [uncultured cnidarian]	6.10^{-10}			Response to stress	HO112288
B-I-190	Selenium binding protein 1	selenium binding protein 1 [Mus musculus]	4.10^{-30}			Immune response	HO112291
B-R-160	Adaptor complexes medium subunit	adaptor complexes medium subunit Domain containing protein, putative [Toxoplasma gondii VEG]	1.10^{-9}			Protein metabolic process	HO112447
B-R-161	Beta-tubulin	beta-tubulin [Pythium sp. quercum]	1.10^{-16}			Cytoskeleton organization	HO112448
B-R-162	Chloroplast phosphoglycerate kinase precursor	chloroplast phosphoglycerate kinase precursor [Euglena gracilis]	2.10^{-33}			Cellular metabolic process	HO112449
B-R-163	Cystathionine beta-lyase	cystathionine beta-lyase [Flavobacteriales bacterium HTCC2170]	9.10^{-6}			Apopotosis	HO112450
B-R-164	Cystatin B	predicted protein [Nematostella vectensis]	7.10^{-8}	cystatin B [Danio rerio]	7.10^{-8}	Immune response	HO112451
B-R-166	Myeloid differentiation response protein 88	hypothetical protein BRAFLDRAFT_81544 [Branchiostoma floridae]	5.10^{-6}	myeloid differentiation response protein 88 [Ictalurus punctatus]	2.10^{-4}	Signal transduction	HO112453
B-R-169	Putative krp3	krp3, putative [Perkinsus marinus ATCC 50983]	3.10^{-4}			Cellular metabolic process	HO112456
B-R-170	major basic nuclear protein	major basic nuclear protein [Karlodinium micrum]	1.10^{-13}			Chromatin remodelling	HO112458
B-R-171	major basic nuclear protein	major basic nuclear protein [Karlodinium micrum]	8.10^{-7}			Chromatin remodelling	HO112459
B-R-172	Mitochondrial phosphate carrier	predicted protein [Physcomitrella patens subsp. patens]	2.10^{-9}	mitochondrial phosphate carrier [Saccharomyces cerevisiae YJM789]	9.10^{-6}	Cellular metabolic process	HO112460
B-R-173	Peridinin chlorophyll-a binding protein apoprotein precursor	peridinin chlorophyll-a binding protein apoprotein precursor [Symbiodinium kawagutii]	1.10^{-16}			Photosynthetic process	HO112461
B-R-174	1-cys peroxiredoxin	GA15914 [Drosophila pseudoobscura pseudoobscura]	9.10^{-18}	1-cys peroxiredoxin DPx-6005 [Drosophila melanogaster]	1.10^{-16}	Response to stress	HO112462
B-R-176	Trypsin	predicted protein [Nematostella vectensis]	8.10^{-30}	trypsin [Marsupenaeus japonicus]	1.10^{-13}	Cellular metabolic process	HO112464
B-R-177	Peptidyl-dipeptidase A	hypothetical protein BRAFLDRAFT_129715 [Branchiostoma floridae]	3.10^{-8}	peptidyl-dipeptidase A [Acidobacteria bacterium Ellin345]	1.10^{-6}	Response to stress	HO112465

B-R-180	Transcriptional adaptor 2	predicted protein [Nematostella vectensis]	2.10^{-40}	transcriptional adaptor 2 [Mus musculus]	8.10^{-16}	Protein metabolic process	HO112469
B-R-181	2-oxoglutarate dehydrogenase	predicted protein [Nematostella vectensis]	4.10^{-17}	2-oxoglutarate dehydrogenase (lipoamide) (e1 component of oxoglutarate dehydrogenase complex) [Schizosaccharomyces pombe]	1.10^{-11}	Cellular metabolic process	HO112470
B-R-183	Similar to damage specific DNA binding protein 1	predicted protein [Nematostella vectensis]	4.10^{-13}	similar to damage specific DNA binding protein 1 [Srongylocentrotus purpuratus]	8.10^{-5}	Response to stress	HO112472
B-R-184	Ribosomal protein S26	predicted protein [Nematostella vectensis]	3.10^{-15}	ribosomal protein S26 [Branchiostoma belcheri]	7.10^{-13}	Protein metabolic process	HO112473
B-R-185	Putative zinc finger protein	PREDICTED: similar to MGC83605 protein [Hydra magnipapillata]	7.10^{-8}	putative zinc finger protein [Euprymna scolopes]	6.10^{-5}	RNA metabolic process	HO112474
B-R-188	60S ribosomal protein L4	predicted protein [Nematostella vectensis]	8.10^{-47}	60S ribosomal protein L4 [Chlamydomonas sp. HS-5]	9.10^{-35}	Protein metabolic process	HO112476
B-R-189	Putative ribosomal protein S21	putative ribosomal protein S21 [Barentsia elongata]	5.10^{-7}			Protein metabolic process	HO112477
B-R-190	Similar to Rab10 isoform 2	predicted protein [Nematostella vectensis]	7.10^{-64}	PREDICTED: similar to Rab10 isoform 2 [Pan troglodytes]	1.10^{-49}	Intracellular protein transport	HO112479
B-R-191	RNA-binding protein	RNA-binding protein [Karlodinium micrum]	3.10^{-13}			RNA metabolic process	HO112480
B-R-194	Thioredoxin domain containing 16	PREDICTED: thioredoxin domain containing 16 [Taeniopygia guttata]	1.10^{-3}			Response to stress	HO112482
B-R-195	Ubiquitin-conjugating enzyme e2-16kda, ubiquitin protein ligase	ubiquitin-conjugating enzyme e2-16kda, ubiquitin protein ligase [Thalassiosira pseudonana CCMP1335]	3.10^{-29}			Protein metabolic process	HO112483
TB-I-172	60S acidic ribosomal phosphoprotein P0	60S acidic ribosomal phosphoprotein P0 [Stylophora pistillata]	3.10^{-53}			Protein metabolic process	HO112666
TB-I-173	Nascent polypeptide-associated complex alpha subunit	nascent polypeptide-associated complex alpha subunit [Pongo abelii]	9.10^{-44}			Protein metabolic process	HO112667
TB-I-175	Calmodulin	Full Calmodulin [Alexandrium fundyense]	1.10^{-78}			Cellular homeostasis	HO112669
TB-I-177	Cytochrome c oxidase subunit I	cytochrome c oxidase subunit I [Stylophora pistillata]	1.10^{-46}			Cellular metabolic process	HO112671
TB-I-178	Ferritin	ferritin heavy chain polypeptide 1 [Branchiostoma lanceolatum]	1.10^{-51}			Immune response	HO112672
TB-I-179	Ferritin	ferritin [Boophilus microplus]	2.10^{-13}			Immune response	HO112673
TB-I-181	Similar to ARP5 actin-related protein 5	hypothetical protein BRAFLDRAFT_118261 [Branchiostoma floridae]	4.10^{-38}	PREDICTED: similar to ARP5 actin-related protein 5 homolog [Macaca mulatta]	9.10^{-27}	Chromatin remodelling	HO112676
TB-I-182	Twinstar	predicted protein [Nematostella vectensis]	3.10^{-11}	twinstar [Drosophila melanogaster]	1.10^{-6}	Cytoskeleton organization	HO112677
TB-I-183	Fibrous sheath CABYR binding protein	hypothetical protein CLOBOL_07325 [Clostridium bolteae ATCC BAA-613]	5.10^{-13}	fibrous sheath CABYR binding protein [Homo sapiens]	6.10^{-9}	Protein metabolic process	HO112678
TB-I-184	Similar to poly (ADP-ribose) polymerase	hypothetical protein NEMVEDRAFT_v1g141705 [Nematostella vectensis]	4.10^{-13}	PREDICTED: similar to poly (ADP-ribose) polymerase family, member 15 [Macaca mulatta]	5.10^{-11}	RNA metabolic process	HO112679
TB-I-185	Similar to katanin p80	hypothetical protein OsJ_16629 [Oryza sativa	2.10^{-4}	PREDICTED: similar to katanin p80 (WD40-	5.10^{-4}	Cytoskeleton organization	HO112680

		Japonica Group]		containing) subunit B 1 [Apis mellifera]			
TB-I-186	TLD domain containing protein	TLD domain containing protein [Plasmodium knowlesi strain H]	5.10^{-4}			System development	HO112681
TB-I-188	Similar to Zinc finger RNA-binding protein	PREDICTED: similar to Zinc finger RNA-binding protein [Bos taurus]	6.10^{-8}			RNA metabolic process	HO112683
TB-I-192	Putative isocitrate dehydrogenase NAD subunit beta	predicted protein [Nematostella vectensis]	3.10^{-14}	isocitrate dehydrogenase NAD subunit beta, putative [Pediculus humanus corporis]	3.10^{-10}	Cellular metabolic process	HO112688
TB-I-193	Major basic nuclear protein	major basic nuclear protein [Karlodinium micrum]	1.10^{-6}			Chromatin remodelling	HO112689
TB-I-194	Major basic nuclear protein	major basic nuclear protein [Karlodinium micrum]	3.10^{-16}			Chromatin remodelling	HO112690
TB-I-195	Precursor of mutase superoxide dismutase [Fe/Mn]	precursor of mutase superoxide dismutase [Fe/Mn] [Phaeodactylum tricornutum CCAP 1055/1]	2.10^{-25}			Response to stress	HO112691
TB-I-196	Putative netrin receptor unc5	netrin receptor unc5, putative [Schistosoma mansoni]	1.10^{-3}			Apoptosis	HO112692
TB-I-198	Peridinin chlorophyll-a binding protein apoprotein precursor	peridinin chlorophyll-a binding protein apoprotein precursor [Symbiodinium kawagutii]	2.10^{-23}			Photosynthetic process	HO112694
TB-I-199	Similar to Transmembrane protein 173	predicted protein [Nematostella vectensis]	7.10^{-6}	similar to Transmembrane protein 173 [Danio rerio]	8.10^{-4}	Immune response	HO112695
TB-I-201	CEBPB (CCAAT/Enhancer binding protein beta) protein	predicted protein [Nematostella vectensis]	5.10^{-14}	CEBPB (CCAAT/Enhancer binding protein beta) protein [Homo sapiens]	4.10^{-4}	Immune response	HO112699
TB-I-204	Hairy A protein	predicted protein [Nematostella vectensis]	1.10^{-24}	hairy A protein [Branchiostoma floridae]	1.10^{-22}	Signal transduction	HO112702
TB-I-205	Concanavalin	predicted protein [Nematostella vectensis]	2.10^{-45}	thrombospondin N-terminal-like domain-containing protein [Synechococcus sp]	2.10^{-4}	Immune response	HO112703
TB-I-206	collagen, type II, alpha 1	predicted protein [Nematostella vectensis]	1.10^{-14}	collagen, type II, alpha 1 [Xenopus laevis]	4.10^{-9}	System development	HO112704
TB-I-207	TRM1 tRNA methyltransferase	predicted protein [Nematostella vectensis]	8.10^{-42}	TRM1 tRNA methyltransferase 1 homolog (S. cerevisiae) [Bos taurus]	1.10^{-33}	Protein metabolic process	HO112705
TB-I-208	Similar to microfibrillar-associated protein 1	predicted protein [Nematostella vectensis]	8.10^{-18}	PREDICTED: similar to microfibrillar-associated protein 1 [Tribolium castaneum]		Immune response	HO112706
TB-I-209	40S ribosomal protein S4	predicted protein [Nematostella vectensis]	3.10^{-42}	40S ribosomal protein S4 [Epinephelus coioides]	3.10^{-25}	Protein metabolic process	HO112707
TB-I-210	Ribosomal protein L19	predicted protein [Nematostella vectensis]	7.10^{-33}	ribosomal protein L19 [Suberites domuncula]	4.10^{-30}	Protein metabolic process	HO112709
TB-I-211	Putative 40S ribosomal protein RPS30	predicted protein [Nematostella vectensis]	5.10^{-26}	putative 40S ribosomal protein RPS30 [Flustra foliacea]	2.10^{-24}	Protein metabolic process	HO112710
TB-I-212	Putative ribosomal protein L18	predicted protein [Nematostella vectensis]	1.10^{-59}	putative ribosomal protein L18 [Barentsia elongata]	6.10^{-59}	Protein metabolic process	HO112711
TB-I-213	Similar to ribosomal protein L35A isoform 2	predicted protein [Nematostella vectensis]	3.10^{-47}	PREDICTED: similar to ribosomal protein L35A isoform 2 [Hydra magnipapillata]	2.10^{-42}	Protein metabolic process	HO112712
TB-I-214	Ribosomal protein S6	predicted protein [Nematostella vectensis]	1.10^{-10}	ribosomal protein S6 [Aedes albopictus]	6.10^{-7}	Protein metabolic process	HO112713
TB-I-215	Argonaute 2	predicted protein [Nematostella vectensis]	1.10^{-13}	argonaute 2 [Oikopleura dioica]	1.10^{-12}	Immune response	HO112714
TB-I-216	Putative 60S ribosomal protein RPL13	predicted protein [Nematostella vectensis]	2.10^{-18}	putative 60S ribosomal protein RPL13 [Novocrania anomala]	1.10^{-16}	Protein metabolic process	HO112715

TB-I-217	40S ribosomal protein SA	40S ribosomal protein SA [Nematostella vectensis]	7.10^{-53}			Protein metabolic process	HO112716
TB-I-218	Similar to 60S ribosomal protein L28 isoform 1	predicted protein [Nematostella vectensis]	3.10^{-44}	PREDICTED: similar to 60S ribosomal protein L28 isoform 1 [Ciona intestinalis]	3.10^{-30}	Protein metabolic process	HO112717
TB-I-219	60S ribosomal protein L13a	predicted protein [Nematostella vectensis]	3.10^{-6}	60S ribosomal protein L13a [Ornithoctonus huwena]	3.10^{-5}	Protein metabolic process	HO112718
TB-I-220	Putative 60S ribosomal protein L38 isoform 1	predicted protein [Nematostella vectensis]	9.10^{-19}	TPA: putative 60S ribosomal protein L38 isoform 1 [Spadella cephaloptera]	3.10^{-18}	Protein metabolic process	HO112720
TB-I-221	Similar to ribosomal protein S6	predicted protein [Nematostella vectensis]	4.10^{-28}	similar to ribosomal protein S6 [Taeniopygia guttata]	2.10^{-27}	Protein metabolic process	HO112721
TB-I-222	Transcript antisense to ribosomal RNA protein 1	hypothetical protein NEMVEDRAFT_v1g155353 [Nematostella vectensis]	4.10^{-24}	Transcript antisense to ribosomal RNA protein 1 [Saccharomyces cerevisiae]	2.10^{-10}	Protein metabolic process	HO112722
TB-I-223	Ribosomal protein 4	ribosomal protein 4 [Lonomia obliqua]	6.10^{-15}			Protein metabolic process	HO112723
TB-I-224	Ribosomal protein L13a	predicted protein [Nematostella vectensis]	8.10^{-23}	ribosomal protein L13a [Suberites domuncula]	3.10^{-21}	Protein metabolic process	HO112724
TB-I-225	Similar to ribosomal protein L34	predicted protein [Nematostella vectensis]	9.10^{-11}	PREDICTED: similar to ribosomal protein L34 [Hydra magnipapillata]	8.10^{-7}	Protein metabolic process	HO112725
TB-I-227	Succinyl-CoA ligase beta subunit	succinyl-CoA ligase beta subunit [Arabidopsis thaliana]	6.10^{-3}			Cellular metabolic process	HO112727
TB-R-149	Acetyl coenzyme A-transferase	acetyl coenzyme A-transferase [Artemia franciscana]	2.10^{-17}			Cellular metabolic process	HO112868
TB-R-151	Calmodulin	calmodulin [Toxoplasma gondii ME49]	7.10^{-70}			Cellular homeostasis	HO112871
TB-R-153	Pdcysteine-rich protein	Pdcysteine-rich protein [Pocillopora damicornis]	3.10^{-25}			System development	HO112873
TB-R-158	RNase NGR3	hypothetical protein [Monosiga brevicollis MX1]	4.10^{-17}	RNase NGR3 [Nicotiana glutinosa]	4.10^{-9}	Immune response	HO112878
TB-R-159	Putative FERM, RhoGEF and pleckstrin domain-containing protein	predicted protein [Nematostella vectensis]	2.10^{-20}	FERM, RhoGEF and pleckstrin domain-containing protein, putative [Pediculus humanus corporis]	2.10^{-10}	Signal transduction	HO112879
TB-R-160	Similar to 60S ribosomal protein L28 isoform 1	predicted protein [Nematostella vectensis]	8.10^{-33}	PREDICTED: similar to 60S ribosomal protein L28 isoform 1 [Ciona intestnalis]	3.10^{-23}	Protein metabolic process	HO112881
TB-R-161	Secreted signalling factor wnt-A	secreted signalling factor wnt-A [Nematostella vectensis]	1.10^{-4}			Signal transduction	HO112882
TB-R-162	Defender against cell death 1	predicted protein [Nematostella vectensis]	8.10^{-18}	defender against cell death 1 [Xenopus (Silurana) tropicalis]	9.10^{-18}	Apoptosis	HO112883
TB-R-163	Similar to Collagen alpha-1(XI) chain precursor isoform 1	predicted protein [Nematostella vectensis]	5.10^{-41}	PREDICTED: similar to Collagen alpha-1(XI) chain precursor isoform 1 [Apis mellifera]	3.10^{-21}	System development	HO112884
TB-R-165	Similar to selectin P	hypothetical protein BRAFLDRAFT_108141 [Branchiostoma floridae]	4.10^{-10}	PREDICTED: similar to selectin P [Taeniopygia guttata]	3.10^{-7}	Immune response	HO112886
TB-R-166	Protein TAR1	predicted protein [Nematostella vectensis]	8.10^{-24}	RecName: Full=Protein TAR1 [Saccharomyces cerevisiae S288c]	5.10^{-10}	RNA metabolic process	HO112887
TB-R-167	Putative translation factor Sui1	translation factor Sui1, putative [Ixodes scapularis]	1.10^{-4}			Protein metabolic process	HO112888
TB-R-169	RNA-binding protein	RNA-binding protein [Karlodinium micrum]	6.10^{-15}			RNA metabolic process	HO112890
TB-R-170	S30-ubiquitin-like	S30-ubiquitin-like [Suberites domuncula]	5.10^{-10}			Protein metabolic	HO112892

						process	
TB-R-171	Subunit of the signal recognition particle	subunit of the signal recognition particle [Chlamydomonas reinhardtii]	9.10^{-3}			Intracellular protein transport	HO112893
TB-R-173	Putative tubulin alpha chain	tubulin alpha chain, putative [Schistosoma mansoni]	1.10^{-3}			Cytoskeleton organization	HO112895
TB-R-174	Ubiquitin ligase 1	ubiquitin ligase 1 [Symbiodinium sp. C3]	4.10^{-21}			Protein metabolic process	HO112896
TB-R-188	Ribosomal protein L23a	hypothetical protein BRAFLDRAFT_121811 [Branchiostoma floridae]	9.10^{-14}	ribosomal protein L23a [Branchiostoma belcheri]	9.10^{-14}	Protein metabolic process	HO112909
BI, bacteria-induced; BR, bacteria-repressed; TBI, thermo-bacteria-induced; TBR, thermo-bacteria-repressed.							